AFRL-VS-
TR-2003-1133

ADVANCED NAVIGATION TERMINAL SYSTEM USING THE GLOBAL POSITIONING SYSTEM

Chris Bartone

Avionics Engineering Center
School of Electrical Engineering and Computer Science
Ohio University
Athens, OH 45701-2979

July 2003

Final Report

AIR FORCE RESEARCH LABORATORY
Space Vehicles Directorate
3550 Aberdeen Ave SE
AIR FORCE MATERIEL COMMAND
KIRTLAND AIR FORCE BASE, NM 87117-5776

AFRL-VS-TR-2003-1133

This report has been approved for publication.

/signed/

SANDRA H. SLIVINSKY, DR IV
Project Manager

/signed/

STEPHEN K. GOURLEY, Colonel, USAF
Chief, Integrated Experiments and Evaluation Division

REPORT DOCUMENTATION PAGE

Form Approved OMB No. 0704-0188

1. REPORT DATE *(DD-MM-YYYY)*	2. REPORT TYPE	3. DATES COVERED *(From - To)*
25-07-2003	Final	15 Aug 01 - 30 Apr 03

Advanced Navigation Terminal System Using the Global Positioning System

5a. CONTRACT NUMBER
F29601-00-C-0212

5b. GRANT NUMBER

5c. PROGRAM ELEMENT NUMBER
63311F

6. AUTHOR(S)
Chris Bartone

5d. PROJECT NUMBER
4793

5e. TASK NUMBER
BM

5f. WORK UNIT NUMBER
AA

7. PERFORMING ORGANIZATION NAME(S) AND ADDRESS(ES)

Avionics Engineering Center
School of Electrical Engineering
and Computer Science
Ohio University
Athens, OH 45701-2979

8. PERFORMING ORGANIZATION REPORT NUMBER

9. SPONSORING / MONITORING AGENCY NAME(S) AND ADDRESS(ES)
AFRL/VSE
3550 Aberdeen Avenue SE
Kirtland AFB, NM 87117-5776

10. SPONSOR/MONITOR'S ACRONYM(S)

11. SPONSOR/MONITOR'S REPORT NUMBER(S)
AFRL-VS-TR-2003-1133

12. DISTRIBUTION / AVAILABILITY STATEMENT
Approved for public release; Distribution is unlimited.

13. SUPPLEMENTARY NOTES

14. ABSTRACT

This report is the final report for the Air Force Research Laboratory (AFRL), Space Vehicles Directorate (SV), Ballistic Missile Technology (BMT) Demonstration under contract F29601-00-C-0212 [1]. This document describes a program where the functional requirements and technical assessment for the development of an Advanced Navigation Terminal System (ANTS) using the Global Positioning System (GPS) were performed. Under the Base Year of this contract, a Functional Level Specification and System (FLSS) Architecture Study were performed. Under Option Year 1, Technology Assessment items on: 1)GPS Transceiver (GPST) and a small All-zenith multipath limiting antenna (AZMLA) was performed. This report documents the outcomes from these activities.

15. SUBJECT TERMS
Global Position System

16. SECURITY CLASSIFICATION OF:			17. LIMITATION OF ABSTRACT	18. NUMBER OF PAGES	19a. NAME OF RESPONSIBLE PERSON
a. REPORT	b. ABSTRACT	c. THIS PAGE			Dr. Sandra Slivinsky
UNCLASSIFIED	UNCLASSIFIED	UNCLASSIFIED	UNLIMITED	52	19b. TELEPHONE NUMBER *(include area code)* 505-846-7222

TABLE OF CONTENTS

LIST OF FIGURES

LIST OF TABLES

Tables

ACKNOWLEDGMENTS

The authors would like to sincerely thank our program sponsor, Dr. Sandra Slivinsky, from the Air Force Research Laboratory, as well as, the Program Technical Director, Mr. Chuck Wilborn, from Aero Thermo Technology, Incorporated.

LIST OF ACRONYMS

AFRL	Air Force Research Laboratory
AGC	Automatic Gain Control
ANTS	Advanced Navigation Terminal System
ARU	Auxiliary Ranging Unit
AS	Air Segment
ASDL	Airborne Segments Data Link
ASU	Air Segment Unit
AZMLA	All-Zenith Multipath-Limiting Antenna
BMT	Ballistic Missile Technology
BPF	Band Pass Filter
C/A	Coarse Acquisition
COTS	Commercial Off The Shelf
DAPL	Differential Airport Pseudolite
DPL	Differential Pseudolite
DTED	Digital Terrain Elevation Data
EM	Electromagnetic
FLSS	Functional Level Specification and System
GPS	Global Positioning System
GPST	GPS Transceiver
GS	Ground Segment
GSDL	Ground Segments Data Link
GSU	Ground Segment Unit
HZA	High Zenith Antenna
IF	Intermediate Frequency
INS	Inertial Navigation System
L1/L2	Link 1 (1575.42 MHz)/Link 2 (1227.60 MHz) for GPS
LAAS	Local Area Augmentation System
LO	Local Oscillator
MLA	Multipath Limiting Antenna
MSL	Mean Sea Level
MSM	Missile System Model
OEM	Original Equipment Manufacture
P-code	Precise-code
PDOP	Position Dilution of Precision
PL	Pseudolite
PRC	Pseudorange Correction
PVT	Position, Velocity, and Time
Rb	Rubidium
RHCP	Right Hand Circular Polarization
RO	Reference Oscillator
SEM	Standard Equipment Module

SS	Space Segment
SV	Space Vehicles
TTL	Transistor-Transistor Logic
UTC	Universal Time Constance
VSWR	Voltage Standing Wave Ratio
WGS-84	World Geodetic Survey-1984

1. EXECUTIVE SUMMARY

This final report documents activities performed under Contract F29601-00-C-0212, for the functional requirements and technical assessment for the development of an Advanced Navigation Terminal System (ANTS), using the Global Positioning System (GPS). Under the Base Year of this contract, a Functional Level Specification and System (FLSS) Architecture Study was performed. Under Option Year 1, Technology Assessment items: 1) GPS Transceiver (GPST); and, 2) a small All-zenith multipath-limiting antenna (AZMLA) were developed. This report documents the outcome from these activities.

Under the FLSS, the ANTS functions are partitioned into Ground Segment (GS), Air Segment (AS), and Space Segment (SS). The ANTS system operates in four primary and five auxiliary modes. The four primary modes are: 1) Mode 1: Differential GPS (DGPS); 2) Mode 2: DGPS / DPL; 3) Mode 3: PL-Only (non-differential with no GPS at some point); and, 4) Mode 4: DPL (No GPS at some point).

After the ANTS (FLSS was largely completed), an Architecture Trade-off Analysis was conducted. A GPS (L1, L2, C/A and/or P-Code) and Inertial Navigation System (INS) integrated system was used as a baseline configuration. This baseline configuration was used to assess if additional performance could be attained for an ANTS. The analysis was largely performed by a Simulation Model using GPS, INS, and Pseudolites (PL)s with an Extended Kalman Filter. The simulations performed modeled an AS trajectory of approximately 535 seconds (8.92 minutes), which uses a 0.7 nmi/hr medium accuracy INS and conservative 4-channel Precise-code (P-code) GPS receiver. An additional four ground-based PL measurements were simulated to provide additional extended Kalman filter measurement updates. Depending on the radial distance of the PL measurements and actual Kalman filter implementation onboard the AS, how the Kalman filter measurements are implemented, and if the PL measurements are available (as simulated in this project) a reduction of horizontal error between 24.6% and 94.7% may be expected with a 68% confidence. Also, altitude error was found to be associated with two factors: a) the radial distance of the PLs, and b) the orientation of the PLs with respect to the AS trajectory. Results show that altitude error reduction between 38.8% and 82.8% may be expected at a 68% confidence (given an optimal onboard (AS) Kalman filter integration). Because of the vehicle dynamics, it is critical that the Kalman filter tuning and measurement update rates, including the overall systems integration of the automated flight controls, be adjusted accordingly to ensure navigation and guidance and control optimization. The final seconds of AS flight (while the space-based GPS is assumed to be not available) are critical to obtain good system performance for the ANTS.

The GPST was formed by integrating an IN500 PL transmitter, a NovAtel Millennium GPS/PL receiver, an RF attenuator/blanker circuit, and a real-time controller, the latter being autonomous and re-configurable. A prototype GPST was developed for applications evaluation in the ANTS and for technology assessment. Due to contractual difficulties with Rockwell-Collins, which did not wish to participate in this development, the secondary source was selected for the PL transmitter. The secondary source, IntegriNautics, Incorporated, provided a larger, highly-capable box (IN500) but generated only L1, C/A, and

P-codes; it did not generate L2 (1227.60 MHz) for GPS. To overcome this shortcoming, a L1-to-L2 translator was designed, built, and tested. The dual-frequency nature of the PL transmitter was used primarily to achieve the desired frequency diversity during scenarios where only one of the two GPS frequencies was available. These PL signals can then be used to augment the GPS Space Vehicles (SV) constellation or be used as a separate ranging source. A low-power version of the attenuator/blanker circuit was designed and built which investigated timing issues associated with the real-time control of this function. Good system performance was attained on L1 and L2, Coarse Acquisition (C/A), and P-code tracking.

Although the overall AZMLA is not complete and did not meet the overall design envelope initially sought, the AZMLA still holds promise to become a mid-range-performing multipath-limiting GPS/PL antenna which can simultaneously operate at both L1 and L2 frequencies. Accurate phase/amplitude response, with this very broad band frequency requirement, is difficult to achieve and will limit sidelobe suppression and the associated desired-to-undesired (D/U) ratio. Preliminary testing of the four-element Cross-V Dipole Multipath-Limiting Antenna (MLA) array indicates that the MLA array alone may be able to provide the desired hemispherical pattern response, which would significantly simplify the AZMLA design, as well as make it smaller and lighter. Control over the vertical patterns of the MLA portion of the AZMLA has proven to be complicated when applying the broad bandwidth requirements upon the array. The design of an adequate Cross-V Dipole, which allows vertical sacking of multiple elements to form a co-linear vertically stacked array, has also been complex. The mechanical layout of the power distribution assembly, in a manner which does not affect the radiation response of the Cross-V Dipole, is problematic. Successful development of the AZMLA is still believed to be possible with additional effort. Further development of the AZMLA is still favorable, given that there is a significant application for an antenna with the performance planned for the AZMLA.

The objective of this program was to provide sufficient assessment for the potential development of an ANTS that will minimize the risk for successful implementation of the final ANTS at some time in the future. Emphasis was proposed and placed on the purchase of Commercial off-the-shelf (COTS) equipment whenever practical and available. The FLSS and the Architecture Trade-off Analysis, although not exhaustive, did provide sufficient detail and illustrated the potential benefit to an ANTS. The GPST developed provided sufficient detail to see the benefit of an integrated GPS-like (i.e., PL) transmitter and GPS/PL receiver package. In addition, the deployment of ground-based PL transmission and reception assets would require a transportable antenna system to mitigate multipath: the AZMLA was a goal of this capability. Though not achieved, it did provide sufficient technology assessment of the small stacked-array prototype. While the overall design predicts good performance, fabrication difficulties existed in terms of mutual coupling between array elements, which limited its overall performance.

For this contractual effort, an FLSS and architecture analysis were documented. Additionally, technology assessments were conducted in key areas which are necessary for ANTS deployment. Several innovative techniques were explored including the development of a GPST, and considering there integrations in multiple Ground Segment Unit (GSUs), and the development of a small AZMLA technology. As stated in the original proposal, all the

major items in the program are "pushing" the state-of-the-art with respect to the fact that, to the best of our knowledge, they are not being done elsewhere. Successful implementations of these techniques will have direct impact on the potential future deployment of an ANTS. Additional risk mitigation would likely be required to ensure this successful implementation.

2. INTRODUCTION

This report is the final report for the Air Force Research Laboratory (AFRL), Space Vehicles Directorate (VS), Ballistic Missile Technology (BMT) Demonstration under contract F29601-00-C-0212 [1]. This document describes the program which performed the functional requirements analysis and technical assessment for the development of an Advanced Navigation Terminal System (ANTS) using the Global Positioning System (GPS). Under the Base Year of this contract, a Functional Level Specification and System (FLSS) Architecture Study was performed. Under Option Year 1, a technology assessment was performed on: 1) GPS Transceiver (GPST) and 2) a small All-zenith multipath-limiting antenna (AZMLA). This report documents the outcomes of these activities.

The development approach originally proposed by Ohio University is summarized as follows:
Phase I: Develop an FLSS for the ANTS that would capture requirements of the AFRL/VS BMT program requirements. This specification would detail the airborne and ground-based subsystems and define a typical scenario that would be used to assess various architectures.
Phase II: An Architecture Trade-off Analysis was conducted that included combinations of GPS and inertial navigation systems (INS), with up to four pseudolite augmentation sources.
Under Option 1 of this contract, a technology assessment for the ANTS applications was to be conducted which include two major components of the ANTS: 1) the development of a GPST, and 2) the development of a small AZMLA technology. Technology of additional items in Options 2, 3, and 4, which included Fast Acquisition and Tracking Block Processing Techniques, ultra-wideband communications technology, and embedded data link technology, were not conducted.

3. PROGRAM OBJECTIVES

The objective of this program was to provide sufficient assessment for the potential development of an ANTS to minimize the risk for successful future implementation of the final ANTS. Emphasis placed on the purchase of commercial off-the-shelf (COTS) equipment whenever practical and available. This report documents the level-of-effort tasks performed in the development of hardware and software that can be used in a prototype ANTS.

4. PROGRAM DESCRIPTION

This Advanced Navigation Terminal System using GPS program documents the functional requirements of AFRL/VS BMT and develops a detailed system architecture analysis and technology assessment of the key items necessary. Several innovative techniques were explored to include the integration of a GPS Transceiver and consider its interaction with other ground-based GPSTs, and to develop small all-zenith multipath-limiting antenna technology. As stated in the proposal, "all of the major items in the program are pushing AZMLA the state-of-the-art with respect to the fact that, to the best of our knowledge, they are not being done elsewhere. Successful implementations of these techniques will have direct applications in the commercial arena including multipath limiting for precise navigation, and GPS ranging applications using the GPST to augment GPS."

4.1 *Overall Concept of an Advanced Navigation Terminal System (ANTS)*

The overall concept of ANTS provides airborne and ground equipment to enable precise position, velocity, and time (PVT) estimation at the sub-2-meter level of the airborne vehicle when GPS is unavailable due to local interference or service disruption. The GPS service disruption could be local or global in nature.

For the ANTS concept, pseudolite (PL) measurements can be thought of as a GPS measurement that is received from ground-based positioning systems instead of space-based satellite positioning systems. The advantage of this is two-fold:

1) Potential for increased accuracy. Since GPS accuracy is a function of the geometry of the measurements, the user now has the luxury or capability to set-up a unique "optimal" geometric ground-based system for an a priori flight path. For example, if altitude accuracy needed to be improved, it may be possible, theoretically, to add pseudolite measurements along the flight path for added vertical navigation position accuracy.
2) Increased availability and modifiability. Frequency, power output, and encrypted modulation technique of the transmitted signal can be tailored for the specific mission at hand and placed in an operational environment much more rapidly than satellites can be placed on orbit.

The ANTS functions are partitioned into a Ground Segment (GS), an Air Segment (AS), and a Space Segment (SS). The ANTS system operates in four primary and five auxiliary modes. The auxiliary modes are modifications to the primary modes that use the Auxiliary Ranging Unit (ARU) to address specific operational scenarios. The GS and AS have associated equipment called the Ground Segment Unit (GSU) and Air Segment Unit (ASU), respectively. This overall concept is depicted in Figure 1. Each air vehicle would have one ASU, while the number of GSUs would be determined by the mode. As illustrated in Figure 1, the AS may have good GPS tracking in its mission, and at some point in time, as it approaches a terminal area, it loses GPS reception. Assuming the AS is using a GPS/INS system for PVT, the GPS/INS system would propagate the PVT solution using the INS only (i.e., coasting). This PVT solution would diverge over time depending upon the quality of the INS unit, the AS dynamics, and the duration of GPS loss. The concept of the ANTS

would be to provide ASU and GSU to enable better PVT precision than would be afforded by the INS-only PVT solution generated by the GPS/INS system.

The GSU and ASU segments consist of subsystems, which are further described in the Functional Level Specification and System [2]. The GSU consists of the GPST containing an Link 1 (1575.42 MHz)/Link 2 (1227.60 MHz) for GPS and a GPS/PL receiver. Components separate from the GPST but still part of the GSU are small transportable high performance multipath limiting antenna (i.e. AZMLA) and associated data link(s). The Master GSU will have two data link functions: 1) the Ground Segments Data Link (GSDL) that is used to communication to/from each of the GSU and the Airborne Segments Data Link (ASDL) (Master GSU only). The other GSUs (non-Master GSUs) will have only operational the GSDL to communicate to other GSUs, but could have a back-up capability to communication to the AS via the ASDL, in which case they would assume Master GSU functionality. The ASU consists of the GPS/PL Receiver, INS, ASDL, and processor subsystems to combine all observable measurement to form a high precision PVT solution.

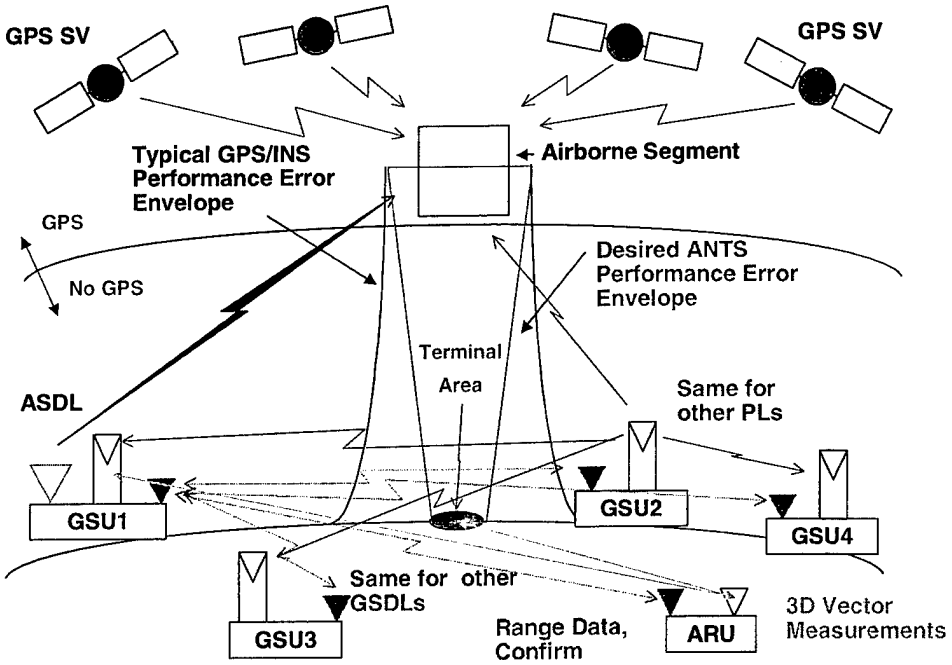

Figure 1. Functional Block Diagram of an ANTS

5. PHASE I

5.1 *Development of the ANTS Functional Level System Specification*

An FLSS was formed which documented ANTS specification items pertaining to scenario definition, GS, GSU, AS, and ASU functionality and operation [2]; these will be summarized here. The scenario definition included the concept of operations of the system, the scope of ground reference sites used to support operations, and performance requirements of the

systems. The AS defines the baseline configuration as a GPS/PL capable L1, L2, C/A and/or P/Y-code receiver with an integrated INS, and it identifies ASDL functionality. The GS definition includes the applicability and capability of various ground equipment to include GSUs and associated GSDL and AZMLA as well as reference points to support ANTS operations.

As part of the ANTS development, an FLSS document was developed. This document defines the functionality and describes the modes, systems and subsystems of ANTS. Additionally, the FLSS document describes the portability and risk analysis of ANTS.

The ANTS functions are partitioned into GS, AS, and an SS. The ANTS system operates in four primary and five auxiliary modes. The auxiliary modes are modifications to the primary modes that use the ARU to address specific operational scenarios. In this final report, only the four primary modes will be addressed, with the auxiliary modes being described in the FLSS document [2]. The four primary modes are:

Mode 1: Differential GPS (DGPS)
Mode 2: DGPS / Differential Pseudolite (DPL)
Mode 3: PL-Only (non-differential, with no GPS at some point)
Mode 4: DPL (No GPS at some point)

Modes 1 and 2 could need as little as one GSU, while Modes 3 and 4 would need at least four GSUs. In all cases except Mode 3, one of the GSUs would be considered the Master GSU. It is envisioned that a two-person crew could eventually deploy each GSU. The GSU would perform a self-survey to determine its location, in either absolute or relative terms, depending on the mode. If the mode depends upon GPS, then the self-survey would be based on the WGS-84 datum set that GPS is based upon.

In ANTS Mode 1, ANTS would operate as a DGPS reference system to augment the PVT accuracy of the AS. A GSU, in DGPS mode with a precisely known location and clock solution, receives GPS signals and transmits pseudorange measurements and coordinates to the Master GSU. The Master GSU then forms an overall pseudorange correction (PRC) for each SV source and then transmits these to the AS, through the data link. This is "basic" DGPS where common error sources are removed and non-common errors are either measured (i.e., ionosphere delays) or modeled (multipath, troposphere delays) and removed.

In a DGPS system, AS PVT accuracy is largely dependent on the geometry of the ranging sources (i.e., GPS SV locations) with respect to the ASU location. Depending on the GPS constellation is operational state and interference environment, the level of availability may not be sufficient to meet the location requirements of the AS in Mode 1. Because of this insufficiency, ANTS Mode 2 includes a DPL along with DGPS. The pseudolite, which is a ground-based "GPS-like" transmitter, augments the satellite constellation to improve the geometry and availability of ranging signals for improved user location PVT performance.

In order to address a dynamic signal-availability environment, in which the GPS signals are either unavailable or denied to the GSU during flight because of jamming, the ANTS Mode 3 operates in a PL-Only mode. In the PL-Only mode the ASU uses ranging signals from the

GSU and SV. However, since no differential corrections are being generated, there is no data link used. Because the location of the PL transmitters and there transmitter clock is needed for AS PVT solution, an operational assumption is made that at some point prior to AS use, the location of the PL transmitter location and their clock solution is solved for. This solution is assumed to be known via GPS with respect to the WGS-84 datum and the clock is propagated using a high quality oscillator (e.g., Rubidium (Rb)).

Mode 4 uses only the PL ranging sources within a minimum of four GSUs and incorporates the capabilities of differential PLs for the solution of the AS PVT. Like Mode 3, Mode 4 involves a scenario in which GPS signals are either unavailable or denied to the GSU at some point within the AS mission. In Mode 4 all of the GSUs forward their observable measurements and self-surveyed coordinated to the Master GSU (software). The Master GSU then computes PRCs for the pseudolite ranging sources within the GSUs, and then transmits these data to the ASU via the data link for AS PVT determination. Mode 4 and all its associated modes depend heavily upon an accurate GSU position and clock solution. Mode 4 must either obtain a surveyed or self-surveyed position using GPS and the WGS-84 datum prior to its becoming unavailable or it must obtain the position survey through alternate means using the ARU.

6. PHASE II

6.1 *Architecture Trade-off Analysis*

After the ANTS FLSS was largely completed, an architecture trade-off analysis was conducted. A GPS (L1, L2 C/A and/or P-Code) and INS integrated system was used as a baseline configuration. This baseline configuration was used to assess if additional performance can be attained for an ANTS.

6.1.1 *Simulation Model using GPS, INS, and Pseudolites (PL)s with an Extended Kalman Filter*

Modeling of an AS trajectory utilizing ground-based PL transmissions for GPS/INS augmentation has not been fully studied. A simulation studying the possible effects of PL measurements near the terminal location was performed to assess the potential benefit of an ANTS [3]. A first-order simulation, based in large-part on previous research [4,5,6,7,8] was performed that included the following modeling:

- AS trajectory that approximates possible mission dynamics, duration and geometric shape
- Post-processed ephemeris data for ranging of the missile GPS receiver and space-based satellite signals
- Four channel P-code GPS receiver
- INS with performance of 0.7nm/hr
- Four ground-based pseudolite aided measurements
- Scenarios where GPS was not available and PLs were used for measurement updates to an extended Kalman filter.

6.1.1.1 Missile Simulation Model (MSM)

The following sections describe the set-up of the computer simulation for the MSM error models. The total number of states for the three navigational subsystems is eighty-seven (87); 39 INS, 30 GPS and 18 PL. Reference [3] contains the details of the error states modeled.

6.1.1.1.1 *Flight Profile Generation*

The flight profile for the missile trajectory was developed by analyzing post-processed data, previously recorded from an actual missile flight test. Once analyzed, a "first-look" missile profile, FLIGHT, was generated using a program PROFGEN [9]. The file FLIGHT contains the information summarized in Table 1.

Table 1. Variables Contained in FLIGHT File

NAME	# OF DIMENSIONS	PROFGEN VARIABLE NAME
time	1	TIME
terrestrial longitude	1	TLON
geographic latitude	1	GLAT
altitude	1	ALT
wander angle	1	ALPHA
roll	1	ROLL
pitch	1	PITCH
yaw	1	YAW
wander angle rate	1	DALPHA
roll rate	1	DROLL
pitch rate	1	DPITCH
yaw rate	1	DYAW
earth velocity in frame n	3	VEN
specific force in frame n	3	FIN

The flight profile computes position, velocity, acceleration, attitude and attitude rate for the AS moving over the earth. Position is given as (geographic) latitude, longitude and altitude. Velocity with respect to earth is coordinatized and presented in a local-vertical frame. Acceleration consists of velocity rates-of-change summed with Coriolis effects and gravity. Attitude consists of roll, pitch and yaw: the Euler angles. The flight profile models a point mass responding to maneuver commands specified by the user.

The AS profile was created by concatenating a sequence of maneuvers, and the resulting output is a binary flight file called "FLIGHT". Appended to the binary FLIGHT file is precision GPS ephemeris data. The ephemeris data was carefully selected based on predicted PDOP values calculated from GPS almanac data that would correspond to Kabul International Airport, N 34.57, E69.21, alt=5871ft. MSL on September 12, 2001. This date corresponds to GPS week #1131, day 255. The SEM almanac data file utilized was: 255.AL3 with the best four satellites based on a minimum PDOP, selected for a missile launch between 19:10 UTC to 19:25 UTC.

The SV's that correspond to the lowest PDOP were SVIDs: 2, 4, 5 and 24. The average PDOP was found to be 3.12 during the missile flight at Kabul. The PDOP for the AS mission duration is shown is Figure 2.

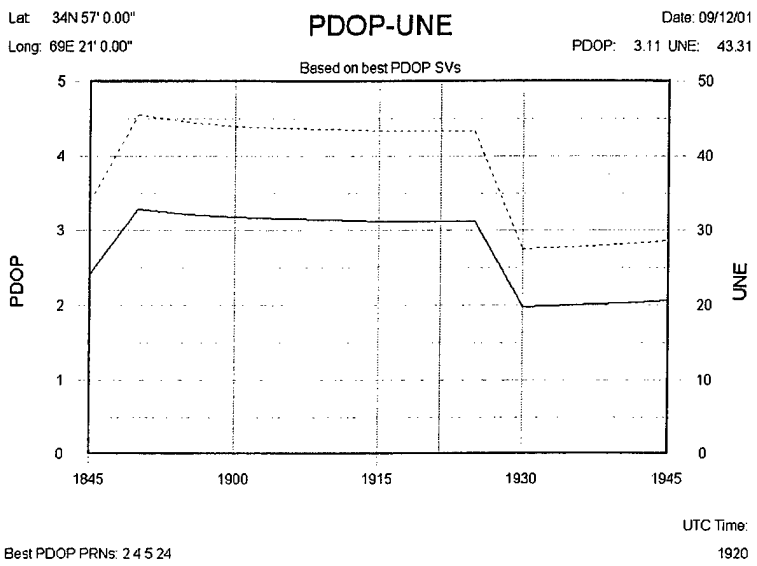

Figure 2. PDOP for Missile Flight Profile Duration

The process of developing a flight profile is summarized below:

- Flight segment template (PROF_IN) created using sample AS trajectory and FLIGHT data file was generated
- Precision satellite ephemeris was appended to the missile FLIGHT profile
- The final FLIGHT file contains the binary flight information, representing the missile trajectory and the precision GPS ephemeris data for each Space Vehicles selected that minimizes PDOP.

6.1.1.1.2 *The INS Model*

A 93-state INS computer model generated and used by past DoD research and later reduced to a 39-state equivalent model was used for this project [4,10,11]. The large 93-state model represents an accurate model available for a ring laser gyro inertial navigation system, but requires a lot of computer processor power and simulation time. While the 93-state model is a very accurate representation of the INS error characteristics, the high dimensionality of the state equations makes the model very CPU-intensive for the scope of this project. The reduced state model is sufficient to investigate an AS profile and specific geographically located ground-based PLs when spaced-based GPS signals are not available.

It should be noted that the barometric altimeter aiding measurements are considered to be INS measurements, while the GPS and PL measurements are the respective updates for the baro/inertial system from the GPS and ground-based PLs.

6.1.1.1.3 *INS Measurement Model*

One measurement commonly used to correct for inherent instabilities of the vertical channel in the filter is the barometric altimeter. The barometric altimeter measurement equation is based on the difference between the INS-predicted altitude, Alt_{INS} and the barometric altimeter-predicted altitude Alt_{Bar}: Therefore it is necessary to develop the two separate measurement signals that will be differenced to attain the proper measurement update for the error state filter. The INS-predicted altitude is the sum of the true altitude, h_t, and the INS error in vehicle altitude above the reference ellipsoid, δh. The barometric altimeter reading is modeled as the sum of the true altitude, h_t, the total time-correlated error in the barometric altimeter, δh_B, and a random measurement noise, v. The difference measurement update signal δz_{Alt} is formed in Equation (1) by subtracting the INS-predicted altitude from the barometric altimeter altitude:

$$\begin{aligned} \delta z_{Alt} &= Alt_{INS} - Alt_{Bar} \\ &= [h_t + \delta h] - [h_t + \delta h_B - v] \\ &= \delta h - \delta h_B + v \end{aligned} \tag{1}$$

6.1.1.1.4 *The GPS Model*

The GPS model is based upon pseudoranges from the GPS receiver equipment [4]. The navigation information passed to the MSM filter is the respective range and ephemeris data position to each of four SVs. A 30-state GPS truth model was used. There are five types of error sources that are modeled in the GPS truth model state equations. The first two states represent the errors in the user clock as range equivalent of user clock bias, and velocity equivalent of user clock drift. The initial state estimates and covariances for these states were chosen to be consistent with previous research [3]. Because these error sources are a function of the user equipment, they are common to all the satellite vehicles. The remaining five sources of errors are unique to each SV, based on their individual equipment and their position with respect to the user. The first SV specific error source is the code loop tracking error, δR_{cloop}. Although the code loop is part of the user equipment shared by all the SVs, its error magnitude is relative to each SV. The second and third SV specific errors are the atmospheric interference with the EM signals, δR_{ion} and δR_{trop}, as related to the ionospheric and tropospheric delay in the signal's propagation. The code loop error, tropospheric delay, and ionospheric delay are all modeled as first order Markov processes with time constants consistent with previous research [5]. All three are driven by zero-mean white Gaussian noise [3]. The fourth SV specific error source is due to inaccuracies in the clocks on board the SVs, δR_{Sclk} and the final error source in the user measurements is based on line-of-sight errors between the SV's and the receiver, δx_{s_i}, δy_{s_i}, δz_{s_i}, respectively. See [3] for additional detail.

6.1.1.1.5 *GPS Measurement Model*

There are four GPS measurement updates, one from each of the SV range signals received by the MSM filter. These measurement updates are once again *difference* measurements. The GPS difference measurement is formed by taking the difference of the INS-calculated pseudorange, R_{INS} and actual pseudorange, R_{GPS}, as shown in Equation (2)

$$\delta z_{GPS} = R_{INS} - R_{GPS} \tag{2}$$

The real pseudorange, R_{GPS} is the sum of the true range from the user to the satellite plus all the errors in the pseudorange signal propagation.

$$R_{GPS} = R_t + \delta R_{cloop} + \delta R_{ion} + \delta R_{trop} + \delta R_{Sclk} + \delta R_{Uclk} - v \tag{3}$$

where

R_{GPS}	=	GPS pseudorange measurement, from SV to user
R_t	=	true range, from SV to user
δR_{cloop}	=	range error due to code loop error
R_{trop}	=	range error due to tropospheric delay
δR_{ion}	=	range error due to ionospheric delay
δR_{Sclk}	=	range error due to SV clock error
δR_{Uclk}	=	range error due to user clock error
v	=	zero-mean white Gaussian measurement noise

The second source of a range measurement is the INS itself, R_{INS}. R_{ins} is the difference between the MSM-calculated position, X_U, and the satellite position from the ephemeris data, X_S. This difference vector is represented below in the ECEF frame:

$$R_{INS} = |X_U - X_S| = \left| \begin{Bmatrix} x_U \\ y_U \\ z_U \end{Bmatrix}^e - \begin{Bmatrix} x_S \\ y_S \\ z_S \end{Bmatrix}^e \right| \tag{4}$$

An equivalent form for Equation (4) is

$$R_{INS} = \sqrt{(x_U - x_S)^2 + (y_U - y_S)^2 + (z_U - z_S)^2} \tag{5}$$

R_{INS} is then linearizied by a first-order Taylor series, with perturbations representing the errors in X_U and X_S:

Finally, the GPS pseudorange truth model *difference* measurement is given as:

$$\delta z_{GPS_t} = R_{INS} - R_{GPS} \tag{6}$$

The user position errors embedded within Equation (6) can be derived from the truth model using an orthogonal transformation. The measurement noise variances for the truth model equations are provided in Appendix B of [3].

6.1.1.1.6 *The PL Model*

The PL truth model contains 18 states to simulate real world errors that are thought to exist in an ANTS. The first two states are common error states, i.e., these errors are common to all ground-based PLs [5] attributed to user hardware. They appear as a bias term and are modeled as random constants as δR_b =Range error due to equipment bias and δv_b =Velocity error due to equipment bias. The initial conditions for the truth model states were chosen to be consistent with [5] and previous PL research [4].

In addition to the common errors when using pseudolites, each of the PLs have four error states to model the unique errors of each one of four PL units. These errors represent the error in the surveyed position (x, y and z) of the PL locations and an atmospheric propagation delay between the PL and the AS PL receiver. The position errors are modeled as random constants and the atmospheric error is represented by a first order Markov process. The details of the error estimate for the PL can be found in [3]. Thus, the truth model for the ground-based PLs, consists of 18 states; two (2) common user error states plus four sets of four (16 total) unique PL error states.

6.1.1.1.7 *PL Measurement Model*

This section describes the truth model measurement equations for the PL updates. Each equation is identical in form for all four ground-based PLs. The PL difference measurement is generated by forming two independent measurements of the range from the PLs to the AS. The extended Kalman filter then takes the difference of these two measurements to form δz. The two range measurements differenced are the INS-computed range (R_{INS}) and the PL-calculated range, R_{PL}:

$$\delta z_{PL} = R_{INS} - R_{PL} \tag{7}$$

The PL range measurement, R_{PL} is the sum of the true range from the ground-based PL to the AS and the errors likely to be found in the measurement signal:

$$R_{PL} = R_t + \delta R_{atm} + \delta R_b + v \tag{8}$$

where:

R_{PL} = PL range measurement from ground-based PL to AS
R_t = true range from pseudolite to missile
δR_{atm} = range error due to atmospheric delay
δR_b = error due to equipment bias
v = zero-mean white Gaussian noise

The second source of range information is provided by the INS. The MSM takes the INS computed position, X_U and subtracts the known OL ground position, X_T. The solution mechanics solved similarly to the GPS difference equation, with the resultant equation actual difference equation between R_{INS} and R_{PL}. The equation for the difference measurement is the complete form of the measurement for the truth model. This equation exactly matches that found in [3].

6.1.2 *Multimode Simulation for Optimal Filter Evaluation (MSOFE)*

All error models described in previous sections make up the user section of the MSOFE simulation [12]. MSOFE is a general-purpose, multimode simulation program for designing integrated systems that employ optimal (Kalman) filtering techniques and for evaluating their performance. For this analysis, 500 Monte Carlo runs were implemented. The simulation was written in ANSI standard FORTRAN 77, and was compiled and run on a SUN ULTRA 1 UNIX computer workstation for this analysis.

6.1.3 *GSU Configuration and Simulation Parameters*

A separate Monte Carlo simulation was run for each different scenario listed in Table 2. A top-view depiction of the AS flight path orientation with respect to the ground-based PLs are shown in Figures 3 and 4. The ground-based PLs are all modeled as being physically located at the same elevation, equally spaced apart from the terminal area center, making a shape of a four-corner square.

Table 2. Monte Carlo Simulation Scenarios

Run #	# of PLs	Flight Path Orientation to Pseudolites	Separation Distance (m)	Time GPS Off Prior to Ground (sec)	Time PL On Prior to Ground (sec)
1	4	Angled	500	60	30
2	4	Angled	1000	60	30
3	4	Angled	2500	60	30
4	4	Angled	5000	60	30
5	4	Straight	5000	60	30
6 (Baseline)	0	***	***	60	***

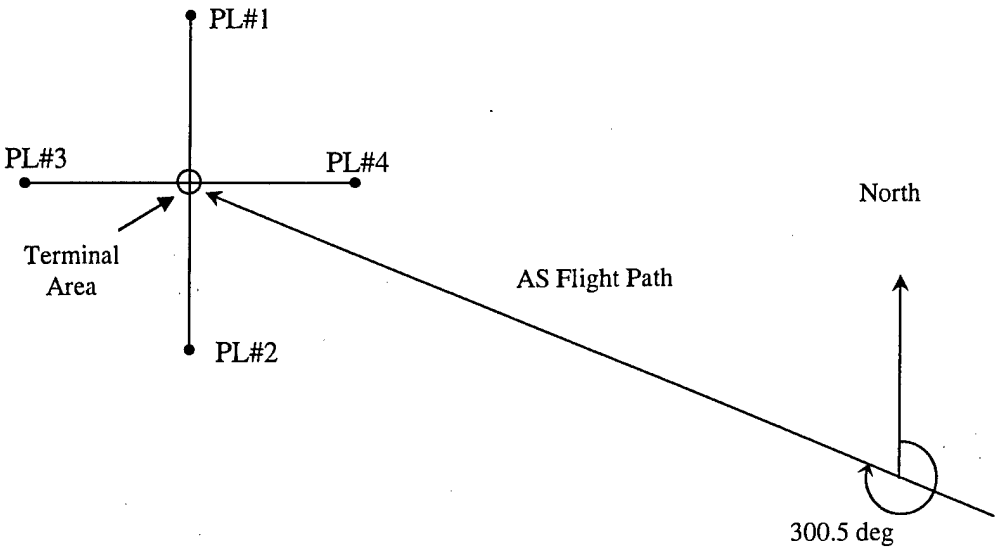

Figure 3. Angled AS Flight Path

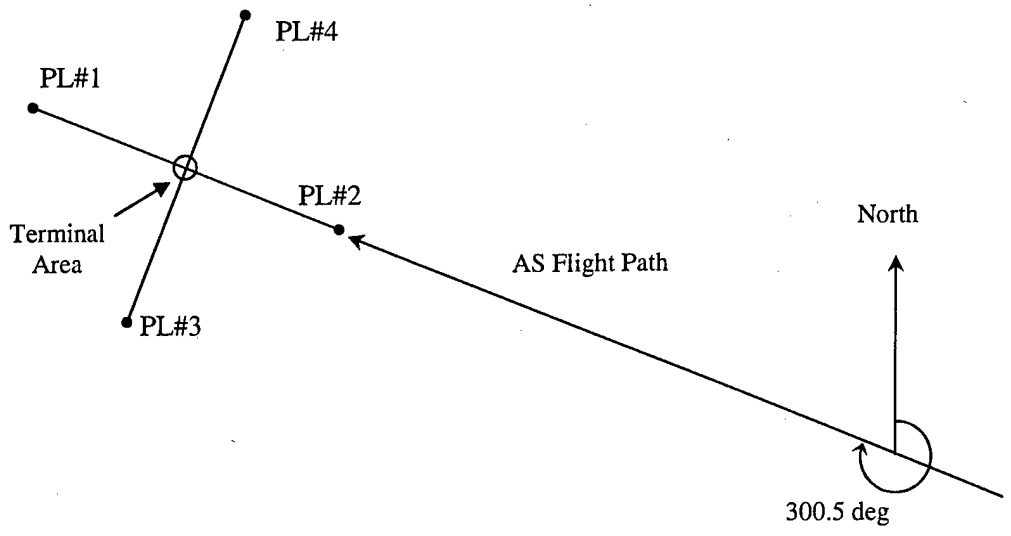

Figure 4. Straight AS Flight Path

6.1.4 *Simulation Results*

In Figure 5, the final ninety-five seconds of the simulation is shown. In this figure, at t=475 seconds, the AS is denied all GPS measurements, simulating the effects of localized interference to GPS for the remainder of the AS flight. The AS continues for an additional 30 seconds utilizing an INS-only means of autopilot control. At t=505 seconds, the AS begins using measurement updates to four ground-based PLs at equal radii apart from the terminal area. The AS continues PL aiding for an additional 30 seconds, until contact with the ground occurs.

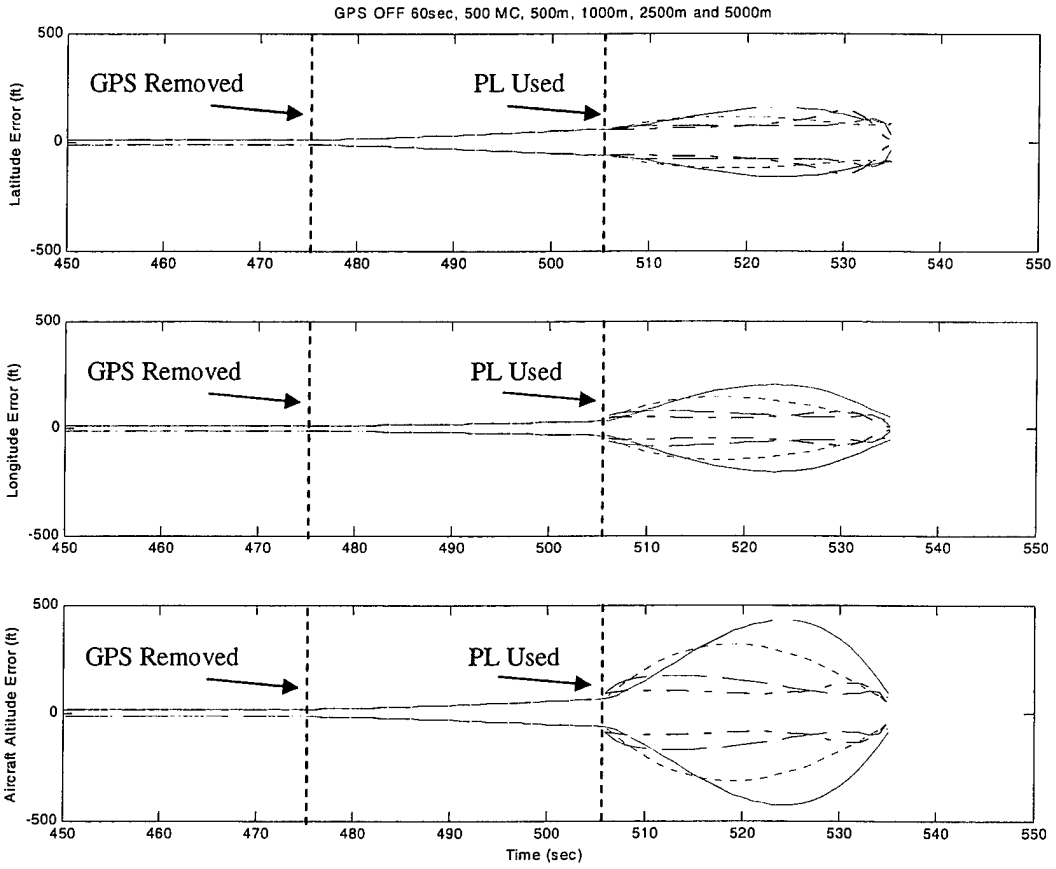

Figure 5. Simulation Runs During the Last 85 Seconds (red solid=500m, green dots=1000m, blue dashes=2500m, black dot-dash=5000m)

Looking at Figure 5, several findings are noted:

- The INS-only period of missile flight performs in graceful degradation with performance matching that of a 0.7 nm/hr system
- At t = 505, all position estimates initially increase when pseudolite measurement aiding is engaged

- The pseudolites spaced farther apart from the target performed better than those that were nearer the target (2500 m & 5000 m performing better than 500 m & 1000 m)
- Altitude error is a dominant source of error
- The latitude and longitude error were not symmetrical, likely due to the incident flight path to the pseudolites being non-symmetrical (330-deg hdg, vs. cardinal hdg PL modeling)
- PL measurements provided the largest increase in aiding during the last portion of the flight
- Need for PL model development to ensure model accuracy

In Figure 6, a comparison between Run 3, Run 4, and the baseline (GPS lost at 60 seconds) is discussed.

In Figure 6, the INS-only degradation is shown as the baseline case. The baseline case does not allow any PL measurement aiding during the entire AS flight. The benefit of PL aiding begins to help decrease altitude error at approximately 10 seconds prior to the ground. In other words, the final ten PL measurement updates decrease altitude errors by approximately 70%. For the PL placement as modeled in this project, horizontal (i.e., in the east, north plane) error reduction does not seem to occur until the final three or four PL measurement updates.

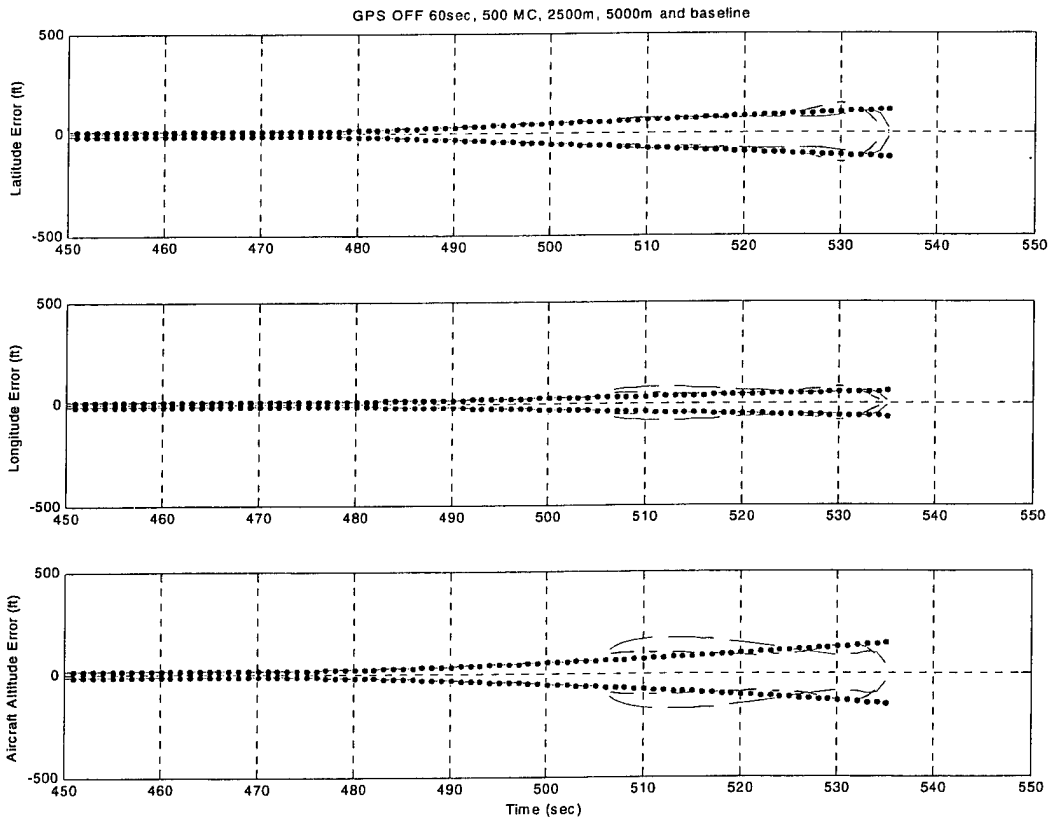

Figure 6. Simulation Runs 3, 4, and Baseline, last 85 seconds (purple dots=baseline, blue dashes=2500m, black dot-dash=5000m)

Looking at Figure 7, which is essentially expanding Figure 6 by zooming in and adding Run 6 (different PL orientation along the flight path), the PL benefit during the final 10 seconds of simulated flight becomes more apparent. Positioning the PLs so that two PLs are aligned with the incoming flight path of the AS depicts aiding to the vertical (elevation) channel, but does not help much in the horizontal plane, when compared with Run 4. Again, all PL run cases were shown to provide aiding during the final AS flight duration.

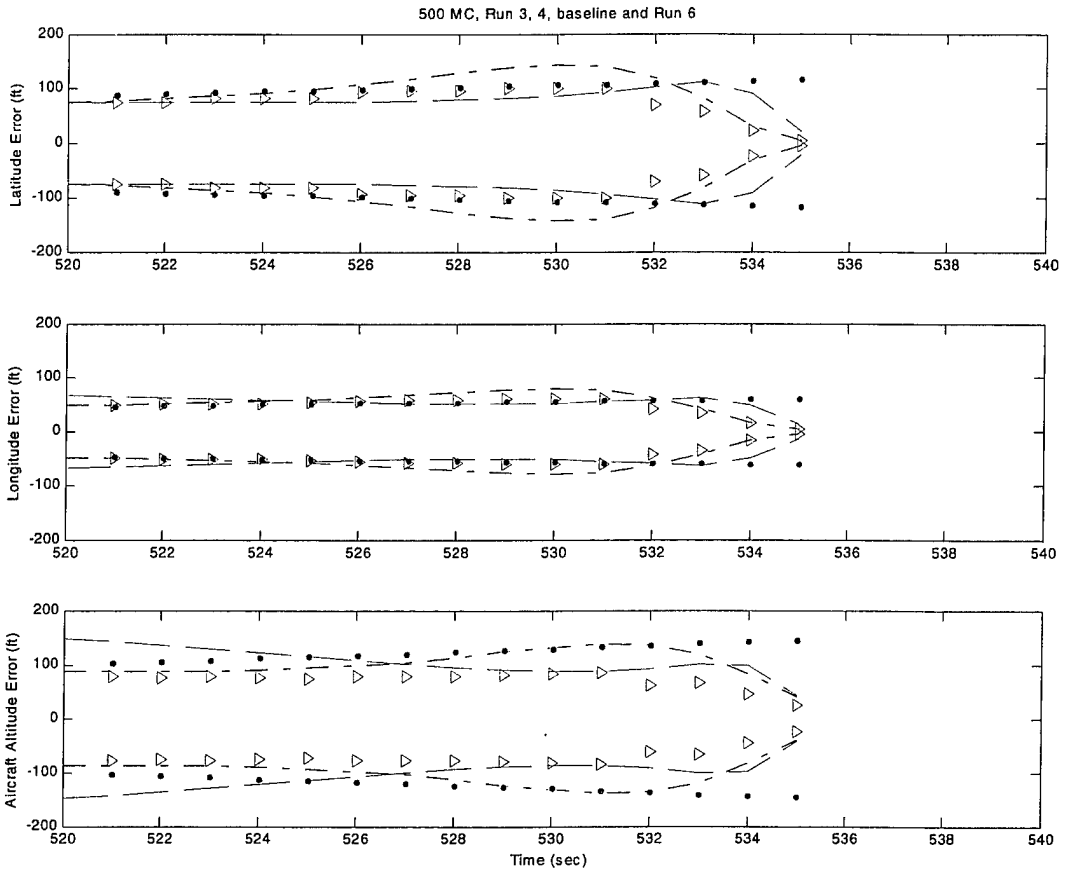

Figure 7. Runs 3, 4, Baseline and Run 6, final 15 seconds prior to impact (purple dots=baseline, blue dashes=2500m, black dot-dash=5000m, cyan triangles=Run 6)

6.1.5 *Data Conclusions*

A summary of PL position aiding benefits at the final impact time is shown in Figure 8. Note that both the radial distance of the PL placed from the terminal area and the actual geometry of the PL placement with respect to the flight path of the incoming AS play a significant role in determining the amount of aiding benefit.

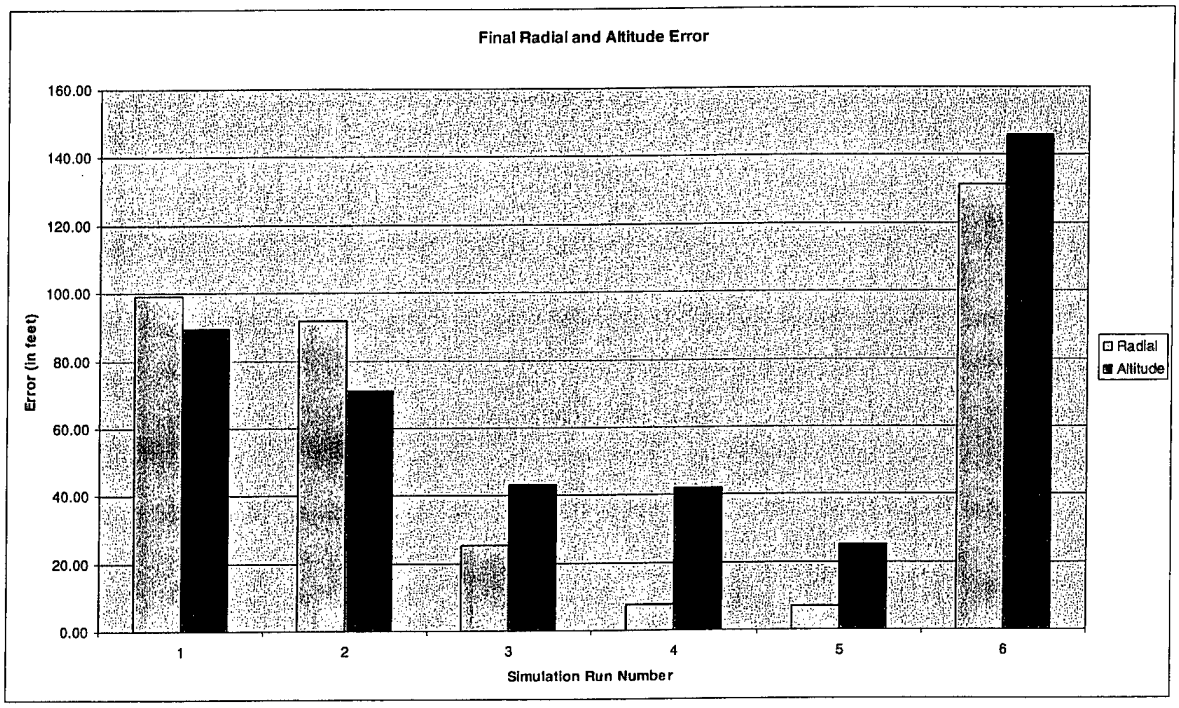

Figure 8. Final Radial and Altitude Error for Simulation Scenarios

Also note that altitude error is only smaller than radial error when the PLs are clustered together less than 1000 m apart. This is due to the PLs being closely spaced in a collinear manner along the AS flight path; otherwise, altitude error remains a dominant source of error when compared with all other cases. A listing of the numerical errors for Figure 8 is shown in Table 3.

Table 3. Final Radial and Altitude Error for Simulation Scenarios (numerical)

Run #	1	2	3	4	5	6 (Baseline)
Radial Error (ft)	99.02	91.65	25.35	7.53	7.01	131.33
Altitude Error (ft)	89.26	70.98	43.23	41.83	25.05	145.89

A listing of the percentage difference for radial error and altitude error between Run numbers 1- 5 vs Run 6 (baseline) is listed in Table 4. For example, when comparing Run 6 (baseline radial error of 131.33 ft) and Run 4 (estimated radial error of 7.53 ft), the percent change in radial error is approximately 94.3% (reduction).

Table 4. Final Radial and Altitude Error for Simulation Scenarios (percentage)

Run #	1	2	3	4	5	6 (Baseline)
Radial Error (% change in error)	24.6	30.2	80.7	94.3	94.7	0
Altitude Error (% change in error)	38.8	51.3	70.4	71.3	82.8	0

6.1.6 *Summary and Recommendations for Simulation Model using GPS, INS, and PLs with an Extended Kalman Filter*

A simulation was performed that models an AS trajectory of approximately 535 seconds (8.92 minutes), which uses a 0.7 nm/hr medium accuracy INS and conservative 4-channel P-Code GPS receiver. An additional four ground-based PL measurements were simulated to provide additional extended Kalman filter measurement updates. All measurement updates from the GPS or PL are in one-second increments.

Depending on the radial distance of the PL measurements and actual Kalman filter implementation onboard the AS, how the Kalman filter measurements are implemented, and if the PL measurements are available, as simulated in this project, a reduction of horizontal error between 24.6% and 94.7% may be expected with 68% confidence. Also, altitude error was found to be associated by two factors: a) the radial distance of the PLs and b) the orientation of the PLs with respect to the AS trajectory. Results showed that altitude error reduction of 38.8% and 82.8% may be expected with 68% confidence given an optimal onboard (AS) Kalman filter integration.

Because of the vehicle dynamics, it is critical that the Kalman filter tuning and measurement update rates, including the overall systems integration of the automated flight controls be adjusted accordingly to ensure navigation, guidance and control optimization. Because of the large error-shape of the curves in Figures 5, 6, and 7, as seen in the final 30 seconds of AS flight (while the space-based GPS is assumed to be not available), the Kalman filter gains and measurement update cycles must be adjusted accordingly to optimize vehicle position certainty.

While their could have been a wide variety of enhancements made to the simulation, which could be implemented in future simulations if required (see list below) the simulation was valuable to show that a ground-based PL network could enhance the position accuracy of an AS for an ANTS.

These possible enhancements include:

- Simulate different PL geometries and locations
- Simulate the benefit of fewer or additional PLs
- Vary measurement update rates
- Vary the time of each GPS outage(s)
- Vary the number of PL measurements allowed at a specific geographic location
- Enhance the PL (very important) or other sensor error models in this simulation by analyzing real (from field measurements) pseudolite error data
- Increase the Monte Carlo runs to > 500
- Refine and enhance the AS profile trajectory
- Study the benefits of PLs, depicting possible threats using DTED data for pseudolite 3-D simulation positioning
- Study Kalman filter gains and measurement update optimization

The results of this study clearly indicate that the final few seconds of the AS flight trajectory are critical and contain the most information for the AS PVT determination.

6.2 *Technology Assessment for an ANTS*

Concurrent with the Trade-off Analysis and Prototyping Phase, the applicability of the following technologies to the ANTS were assessed:

1. GPST configuration will be a factor with respect to making this transceiver portable enough to support a deployable ANTS. As believed prior to contract award, the current size of a GPST like system is larger than that defined in Task 1.0 of this contract.
2. Small All Zenith Multipath Limiting Antenna (AZMLA) technology that will have good hemispherical coverage and good desired-to-undesired (D/U) ratio of approximately 20 dB.

6.2.1 *Technology Assessment for GPST Technology*

Since 1994 Ohio University has been involved with the development of airport pseudolites (APL) for the FAA-sponsored Local Area Augmentation System [13,14,15,16]. This development has been for both on-L1 (1575.42 MHz) and off-L1 operation, C/A and Wideband (Modified P-code) using multipath limiting antenna technology. An APL was successfully integrated into a high-accuracy DGPS/DAPL position solution, which increased the availability of the GPS constellation [17]. Ohio University developed two GPSTs to assess this technology for applications in the ANTS. The AZMLA and data link functions are considered to be outside of the GPST functionality.

6.2.1.1 *GPST Overview Description*

By integrating a PL transmitter and a GPS/PL receiver the GPST is formed; the system is autonomous and re-configurable. The data link that supports GSU-to-GSU and Master GSU-to-ASU communications is considered separate from the GPST. A prototype GPST was developed for applications evaluation in the ANTS and for technology assessment. As illustrated in Figure 9, each GPST is controlled by a PC in a PC-104 form factor running a real-time operating system. A QNX (UNIX like) real-time operating system (OS) was selected and used for this controller function. An alternative real-time OS could also work for this function (e.g., Linux, VxWorks, etc.) For ease of testing, each component of the GPST was developed separately. Prior to option award, a the Rockwell L1,L2, C/A and P-code simulator card was selected to be the PL transmitter. Due to contractual difficulties with Rockwell-Collins, which did not wish to participate in this development, the secondary source was selected. The secondary source, IntegriNautics, Incorporated, provided a larger, highly capable box (IN500) but was L1 C/A and P-code only; it did not generate L2. To overcome this shortcoming, an L1-to-L2 translator was designed, built and tested. The dual-frequency nature of the PL transmitter was used primarily to achieve the desired frequency diversity during scenarios when only one of the two GPS frequencies was unavailable due to possible interference. These PL signals can then be used to augment the GPS SV constellation or be used as a separate ranging source. Each GPS and PL receiver is capable of receiving L1, L2, C/A and P codes. The GSDL for each GPST enables communication between multiple GPSTs in a simulated local area (e.g., bench testing). The datalink

functionality was incorporated via a Freewave wireless RS-232 device, which is frequency hopping in the 900 MHz band.

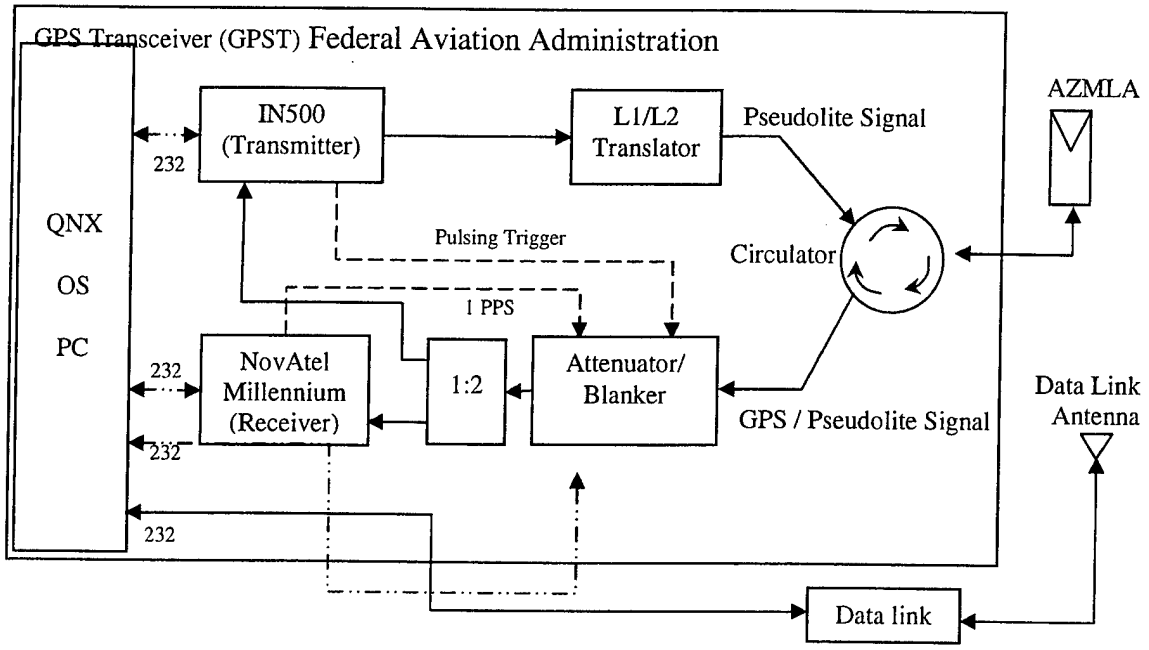

Figure 9. GPST Block Diagram and Associated AZMLA and Data Link

6.2.1.2 *PL Transmitter*

The original equipment manufacture (OEM) version of the IN500 PL transmitter is shown in Figure 10. Figure 11 illustrates the unit in a 19" rack test configuration. Both units are low power (P_t = 13 dBm) versions of the IN500 transmitter. The PL generates L1 C/A and P-codes signals, which can be synchronized with the GPS constellation when available as shown in Figure 9. This synchronization allows the PL transmissions to be continuously synchronized in time with GPS time. The IN500 performs a filtered GPS time solution and continuously adjusts the PL time-of-transmission (TOT_{PL}). In the original OEM version of the IN500 if the GPS signals are lost signal transmission would halt. One change made in this project was to allow the IN500 to transmit PL signals continuously even if GPS service is disrupted. The transmitter TOT_{PL} would drift over time, at the rate of the internal Rubidium reference oscillator (RO), but would be corrected for by the Master GSU to allow time synchronization of the ground-based PL. A pulse trigger output of the IN500 was used as an input to a dynamic attenuator/blanker to "turn-down" the PL transmission power only during the time when the PL transmitter was on. When the PL transmitter was off, the attenuator/blanker would be set to zero, allowing for GPS signal reception. When GPS was deemed to be unavailable and interference was detected by the GPS/PL receiver, then the attenuator/blanker is set to 63 dB, thus allowing additional anti-jam protection to the PL receiver. This technique is sometime called "anti-blanking.

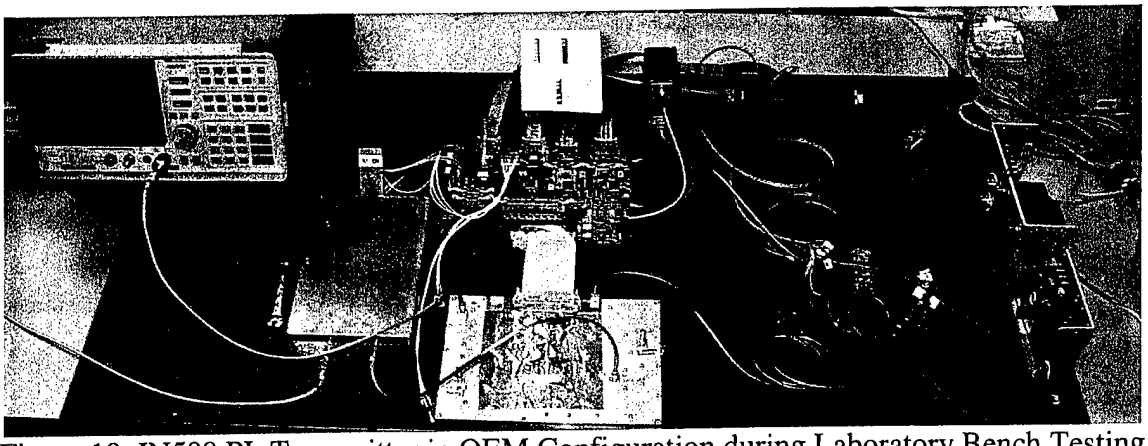

Figure 10. IN500 PL Transmitter in OEM Configuration during Laboratory Bench Testing

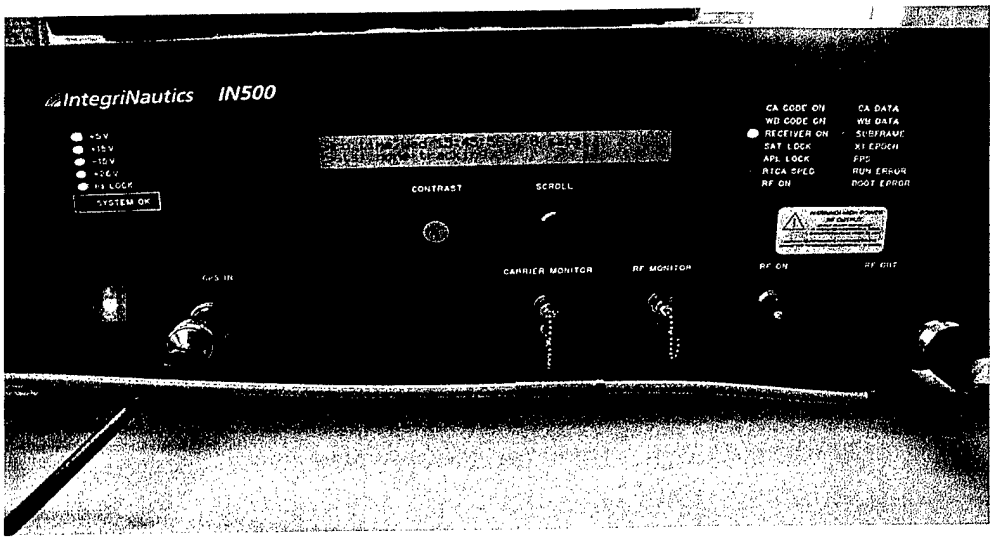

Figure 11. IN500 PL Transmitter in Test Rack Configuration

The OEM PL generates a single frequency output on the GPS L1 frequency (1575.42 MHz). To enhance system performance in terms of frequency diversity, provision of a second PL frequency on the GPS L2 frequency (1227.6 MHz) was implemented with an L1/L2 translator as shown in Figure 12. The L1-to-L2 Translator provides the PL signal on L2 as well as the original L1 frequency. Translation was accomplished by splitting the PL signal so that one signal can be down-converted, while the other remains at the L1 frequency. With the input to the translator as the PL signal at + 10 dBm, via the IN500 Pseudolite, the signal should not need to be band-pass filtered at L1 if the power density at the image frequency (1227.6 - 347.82 = 879.78 MHz) is sufficiently low. After testing, significant power was present at these frequencies (-60 dBm), so an L1 band pass filter (BPF) was implemented. The L2 BPF is used to reduce signal on the sum product produced at 1923.24 MHz. The L1 and L2 signals are then recombined to form the final PL signal for use in the GPST.

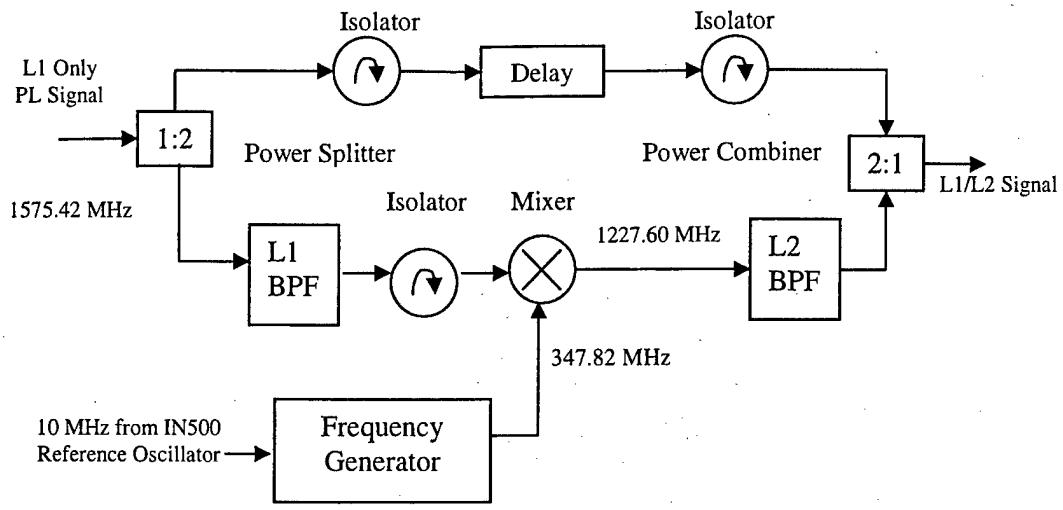

Figure 12. L1-to-L2 Translator Block Diagram

In order to provide some input power margin at the 1 dB compression point, a mixer level of 17 was selected (14dB input for 1 dB compression). Practically, the mixer should be connected in a way that maximizes local oscillator (LO) and L1 input signal suppression at the output. This was accomplished by connecting the L1 input to the RF port, the LO to the IF port, and taking the output L2 signal from the LO port and thus maximizing the input vs output isolation. The worst case isolation for each: LO-RF and LO-IF is 20 dB while the best case is 25 dB. For initial testing purposes, a signal generator provides the required 347.82 MHz LO for downconversion into the double balanced mixer. Later in testing, the LO signal was generated with a small Communication Techniques (CTI) synthesizer clocked by a 10 MHz Rb RO, in the IN500.

The output of the mixer is then band-pass filtered (BW = 24 MHz, 3 dB bandwidth) to remove higher order mixer harmonic at 1923.24 MHz. The L2 signal and the original L1 signal are then recombined into a composite L1/L2 signal via a combiner. The translated path will have an induced phase/group delay as a result of the additional components and feedline. This can be compensated for (via a delay) by adding additional feedline length on the L1 pass-through side.

The L1/L2 translator was shown to function properly. This testing was accomplished by using a PL capable NovAtel Millennium receiver to acquire both L1 and L2 C/A code signals. After an initial settling period (a few minutes), the receiver acquired the L2 signal and tracked both L1 and L2 signals without problem and was then able to hand over to the P-Code (delayed version). The receiver was able to continue tracking the composite PL signals for the entire duration of testing (several hours).

6.2.1.3 *GPST Attenuator/Blanker*

Since the PL signal is generated on the GPS L1/L2 center frequency it must be pulsed in order to prevent interference to GPS receivers. In addition to pulsing the PL signal within the GPST the composite GPS/PL RF path to the receiver must be attenuated to prevent saturating the GPS/PL receiver with too much power. Figure 13 is a block diagram of the GPST Blanker/Attenuator circuit prototyped. The IN500 PL performs pulsing of the transmitted signal and a local version of this pulsing format is available on a parallel-type port on the unit. This pulsing format output is used to drive the attenuator/blanker component, which is placed prior to the NovAtel GPS/PL receiver and the internal GPS/PL receiver within the IN500 PL generator (used for GPS time synchronization). One issue to using the pulsing output of the IN500 is timing latency of this output with respect to the actual RF signal time output. The baseband output is at a TTL signal with a 4.5 V "high" level. Timing analysis was performed and showed that the internal PL RF pulses lag those of the baseband PL pulser output by 356 ns. This latency could greatly increase if the attenuator blanker driver circuit isn't carefully designed. Too much latency would allow high power PL signals to enter the local GPS/PL receivers and push the automatic gain control (AGC) circuits out of range to receive normal GPS signals. An alternative approach may be to tap off the baseband pulsing format earlier internal to the IN500. Further testing is needed in this area to ensure proper operation with low risk of failure.

Rapid blanking is provided by two cascaded GaAs high isolation switches, which are triggered by the baseband PL pulser output. Low power versions were implemented here, however further development would require higher power versions to handle increased power commensurate with the final power transmitted by the PL. Each switch was shown to provide 62 dB of on/off isolation, thus provide 124 dB of isolation when cascaded. Some RF leakage (-51dBm to -31dBm) is present on each of the baseband control ports of the switch so a low-pass filter was added to increase this isolation. The switches require a bipolar +/- 8 Volt control voltage so the attenuator/blanker has a driver circuit added. A simple driver circuit was implemented to provide blanker functionality, but a more robust design is required with less latency for a final design. A high-speed variable attenuator is also placed in the attenuator chain to provide dynamic power level control to allow the user to dynamically adjust the power level to the GPS/PL receivers. This functionality has not been implemented at this time and would require some additional control circuitry.

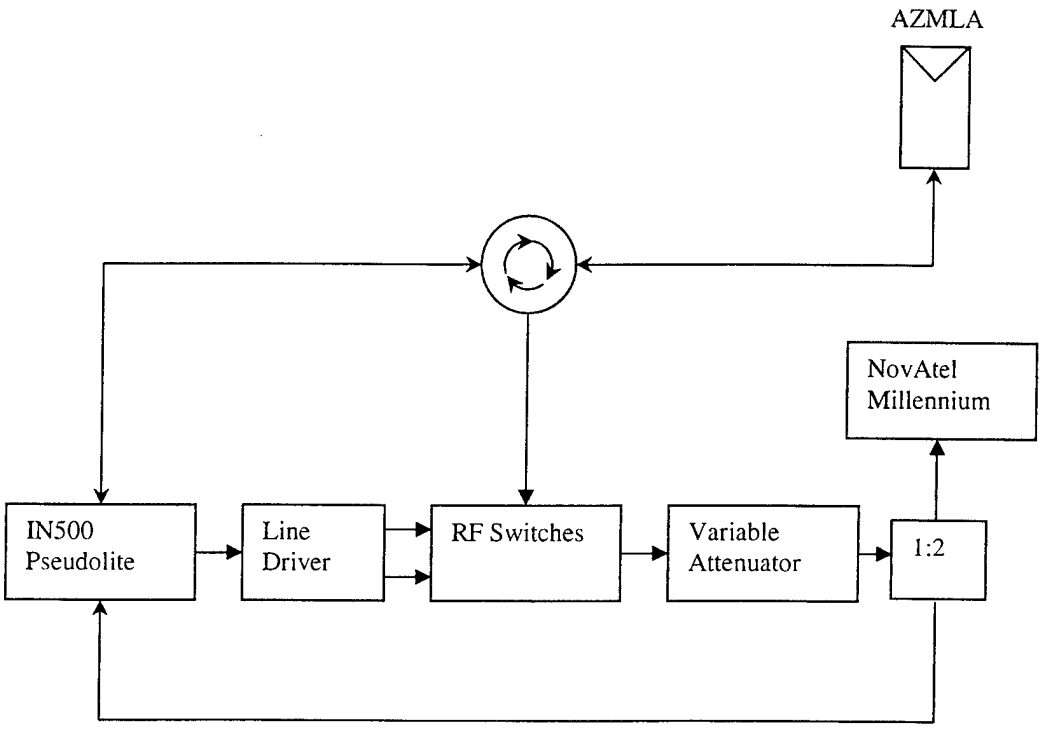

Figure 13. Cascaded High-Isolation Switch Circuit and Attenuator for the GPST Attenuator/Blanker

6.2.1.4 *NovAtel Millennium GPS/PL Receiver*

Three Millennium receivers were updated with newly developed GPS/PL software to allow the reception and processing of the PL signals; Figure 14 is a photograph of a Millenium receiver in a protective enclosure. These receivers were tested in the laboratory and the field for many hours and they operated as expected. The receiver interfaced with the PC104 control PC, which provided control and data collection. The receiver's local oscillator was synchronized with the PL Rb RO via an external oscillator input to increase TOT_{PL} accuracy. Connection to the Rb RO has the advantage allowing better TOT_{PL} residual determination. That can be passed on the GSDL to allow other GSUs more rapid PL direct-P code acquisition, a technique that is used in the Ohio University prototype version of the Local Area Augmentation System (LAAS), [18]. Additionally, when GPS is unavailable the GPS/PL receiver clock drift will be bound by the stability of the Rb RO, which will enable more rapid acquisition than a crystal-based RO.

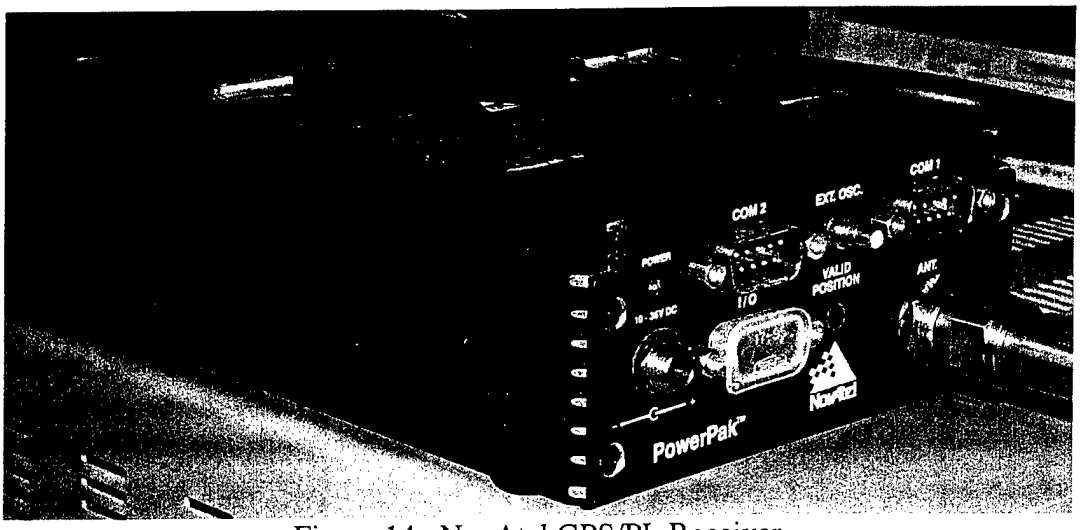

Figure 14. NovAtel GPS/PL Receiver

6.2.1.5 *PC104 Control Computer*

A PC104 computer was assembled with six serial ports used to interface with all the hardware within the GPST the computer was installed in a rigid enclosure, see Figures 14a and 14b. This computer was configured with the QNX real-time OS in order to control all of the hardware. Receiver interface and data collection software was tested and shown to work reliably.

Figure 14a. PC104 Controller Computer


Figure 14b. PC104 Mounted in Enclosure

6.2.2 *Technology Assessment for an All-Zenith Multipath-Limiting Antenna Technology (AZMLA)*

In a ground supported DGPS or differential DPL augmentation system, low-frequency ground multipath is a dominant error source. The design challenge under this task was to provide a sharp roll-off of the elevation radiation characteristics, and sustain full hemi-spherical coverage. Since 1991, Ohio University researchers have been striving to develop a high performance multipath limiting antenna design to support precision approach

applications. From 1994 to 1998 a practical antenna system was developed by Ohio University in support of the FAA Local Area Augmentation System, which consisted of two separate antennas; see references [19]. The goal under this program, was to develop a single antenna that is relatively small (one-man transportable) that has reasonably good performance (~20 dB D/U) over all elevation angles (~5 deg up to zenith (90 deg)). A plot of the desired elevation radiation pattern characteristics is shown in Figure 15. The antenna is planned to have an omni-directional pattern in azimuth.

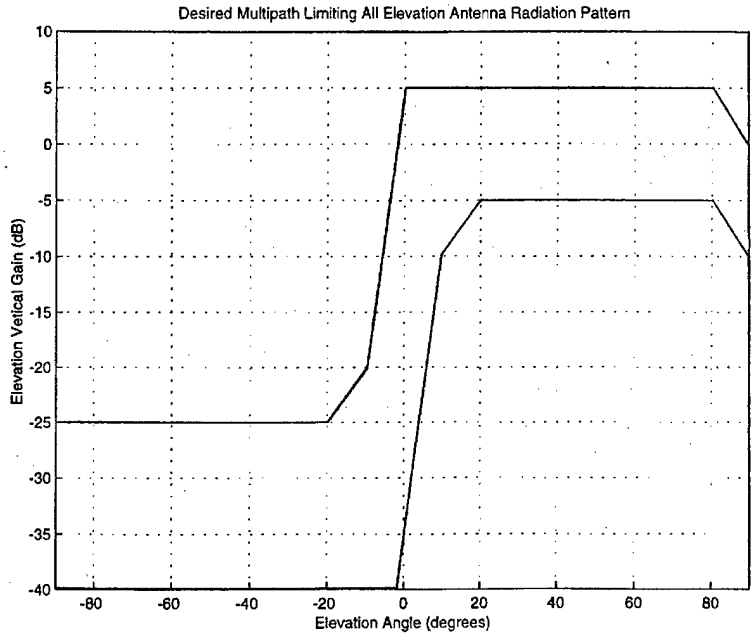

Figure 15. Desired AZMLA Elevation Coverage Zone
(This may need refined to build a portable unit.)

6.2.2.1 *AZMLA Details*

Development of the AZMLA is not complete because the technical challenges of AZMLA development are greater than originally planned. Successful development of the AZMLA is believed to be possible and still shows promise. The data that follow summarize the current status of the AZMLA development and performance. These data are more fully documented in [20]

6.2.2.2 *Voltage Standing Wave Ratio (VSWR)*

Over the frequency band from L2 (1227) to L1 (1575) good input impedance match for the AZMLA is required for acceptable antenna efficiency and performance. The VSWR was measured from 1150 MHz to 1600 MHz for a continuous VSWR measurement at the input to each cross-V dipole. A typical VSWR plot for this input impedance response can be found in Figure 16. The VSWR of each cross-V dipole exhibits a VSWR of less than 1.6:1 over the frequency band of operation. These impedance data indicate that the antenna element may

also provide adequate performance at the new GPS L5 frequency. It should be kep in mind that the overall input impedance of the AZMLA should improve at the main and final input of the AZMLA main power and phase distribution assembly. This good VSWR will provide some additional isolation from the impedance mismatches originating from the cross-V dipole RF feed points.

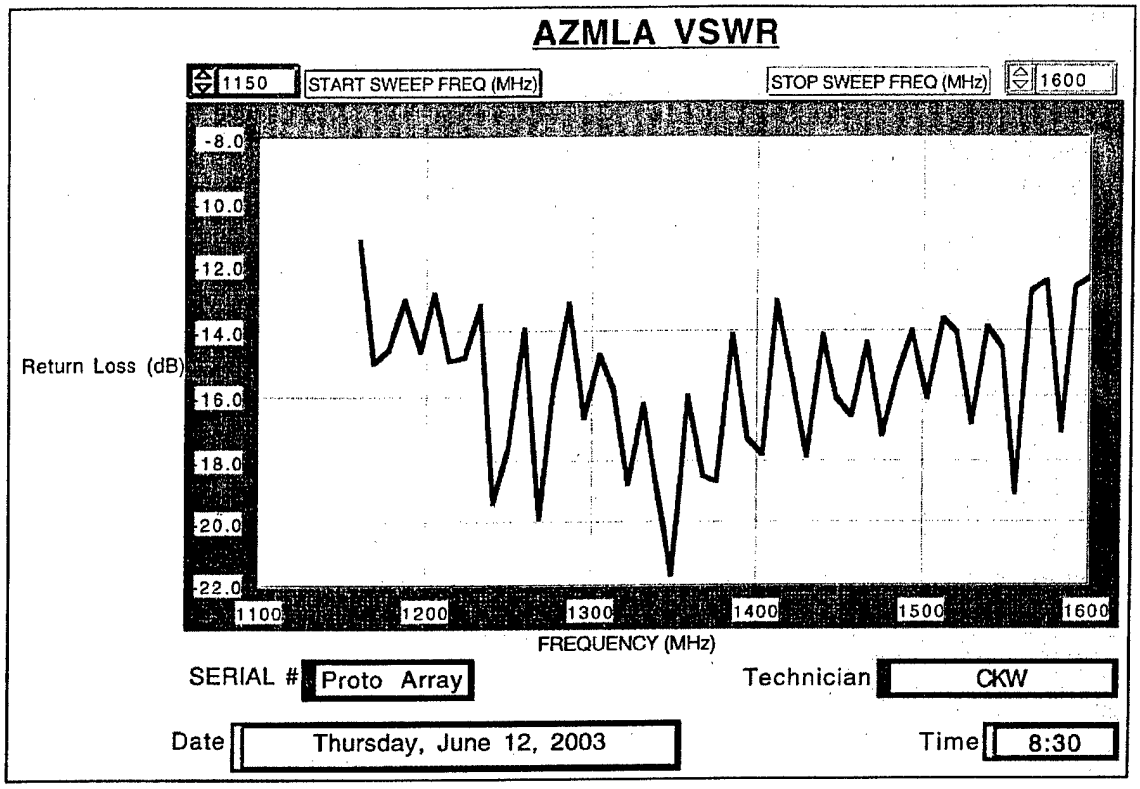

Figure 16. AZMLA VSWR

6.2.2.3 *MLA Portion of the AZMLA*

Significant effort has been expended on the development of a cross-V dipole element, which will provide the desired impedance and radiation performance for the MLA portion of the AZMLA. The same cross-V dipole planned for use in the MLA is also being used as the principal radiator in the HZA. This dual use of the primary radiating element is important when pattern vector summation is performed between the MLA and the HZA. If the elements used in the HZA and the MLA are not equally matched in amplitude and phase response, the combined patterns will result in nulls within the coverage volume.

An eight-element MLA array has been constructed as originally designed. Photos of the eight-element MLA array are shown in Figures 17, 18, and 19. The copper metal center support structure includes four frequency-matched baluns* for each cross-V dipole (one for each dipole arm) which are machined into the center support tube which provide a high

* balun – abbreviation for balance and unbalance; it is a device that interconnects an unbalanced coaxial line to a two-conductor line.

impedance to the input feed points. These baluns help provide a good input impedance match to the feed points of the cross-V dipole and force it to radiate outward onto the radiators. The radiators used on the cross-V dipole are in the shape of wide conical triangles. This conical triangular shape was conceived by the researchers at Ohio University. This unique shape aids in the creation of a very wide operational frequency bandwidth. The white PVC pipe frame is simply a support structure used for antenna range testing and it provides easy access to the MLA array during prototype work. Figure 20 shows the 90-deg hybrid devices used at the feed to each cross-V dipole, which create the Right Hand Circularly Polarized (RHCP) radiation patterns from the dual-linear polarization response of the cross-V dipole element. Each of the eight elements in the MLA array utilizes a 90-deg hybrid device which is located inside the center support tube. The 90-deg hybrid devices are fed with the MLA's power and phase distribution assembly, which is shown in Figure 21.

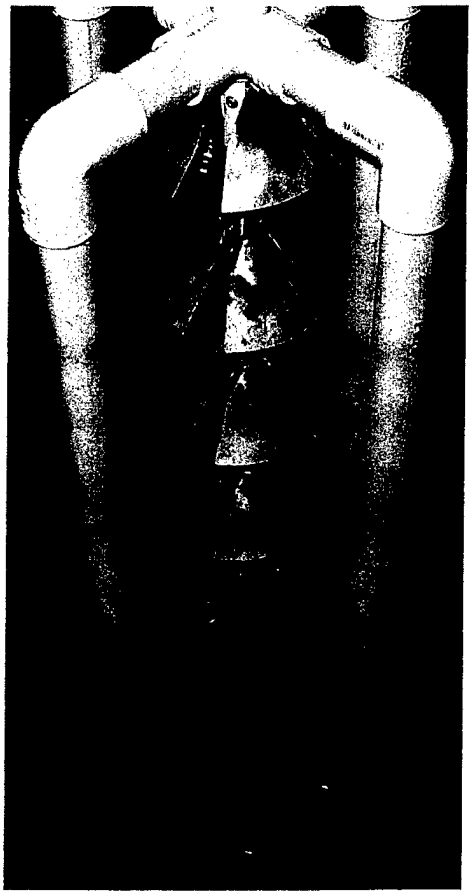

Figure 17. MLA Eight-Element Array

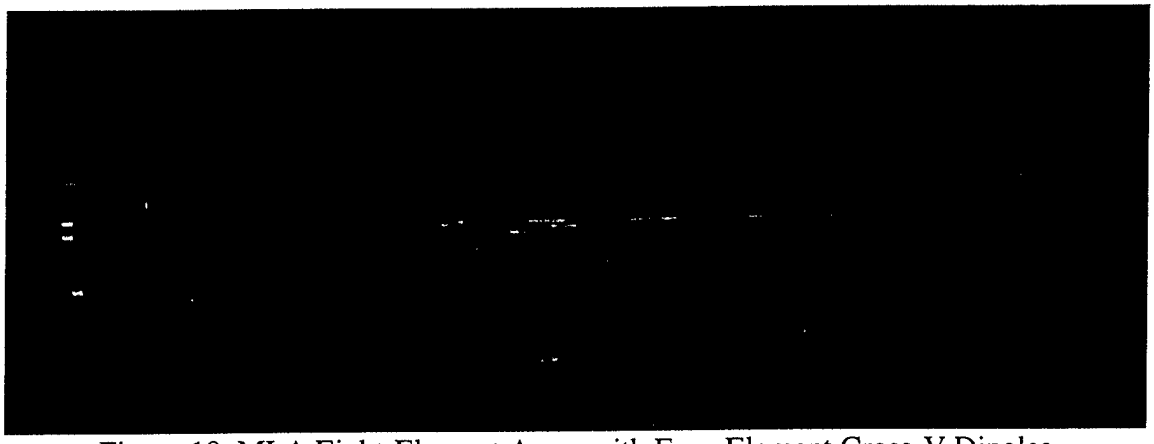

Figure 18. MLA Eight-Element Array with Four-Element Cross-V Dipoles

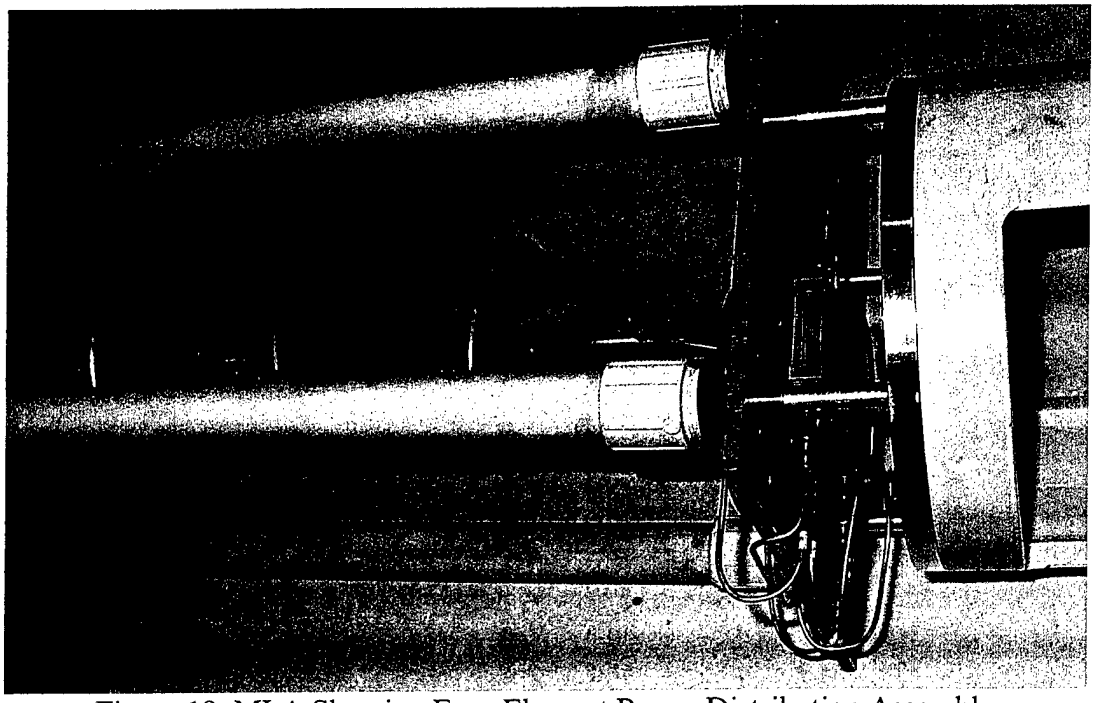

Figure 19. MLA Showing Four-Element Power Distribution Assembly

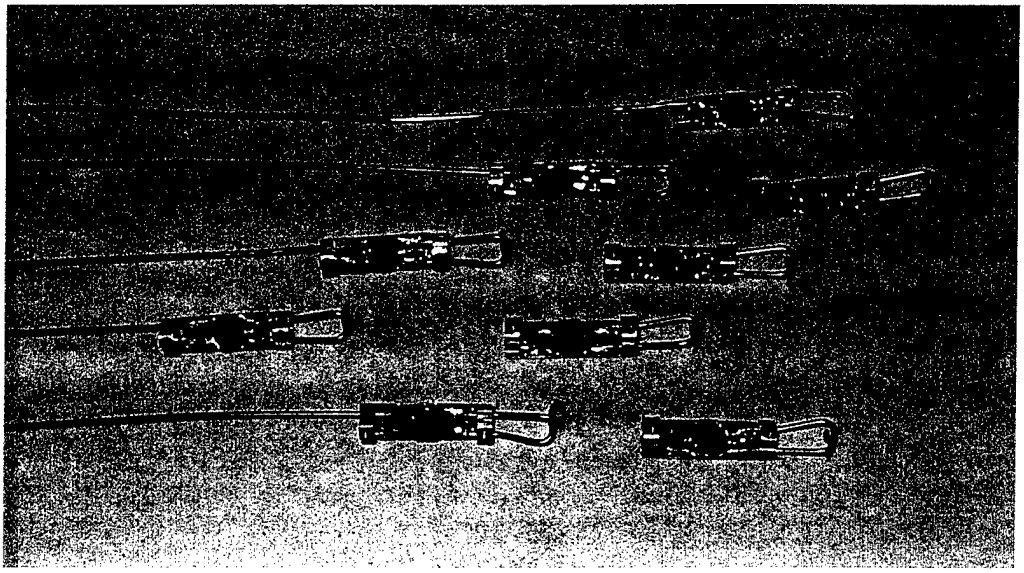

Figure 20. 90-deg Hybrid Power Splitters

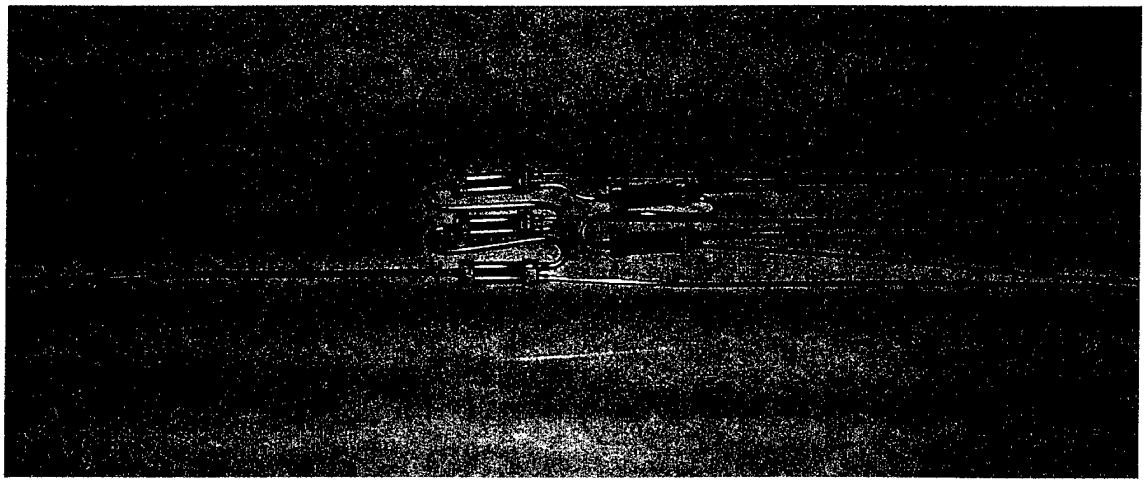

Figure 21. Eight-Element Power Distribution Assembly

6.2.2.4 *MLA and MLA RF Carrier Vertical Radiation Patterns*

The vertical (i.e., elevation plan cuts) RF Carrier radiation patterns for the AZMLA MLA Cross-V Dipoles have been measured at L1 (1575 MHz) and L2 (1227 MHz). Vertical radiation patterns for the following configurations are included in this report:

- One of Eight Cross-V Dipoles fed in the center of the radiating array. These data help quantify the elemental pattern response of the cross-V dipole when located within the eight element array. Knowing the elemental pattern response of the primary cross-V dipole used in the array is critical in the overall array pattern synthesis, which is required to shape the eight-element pattern. The RHCP vertical patterns recorded at L1 and L2 for the single element response are shown in Figure 22.

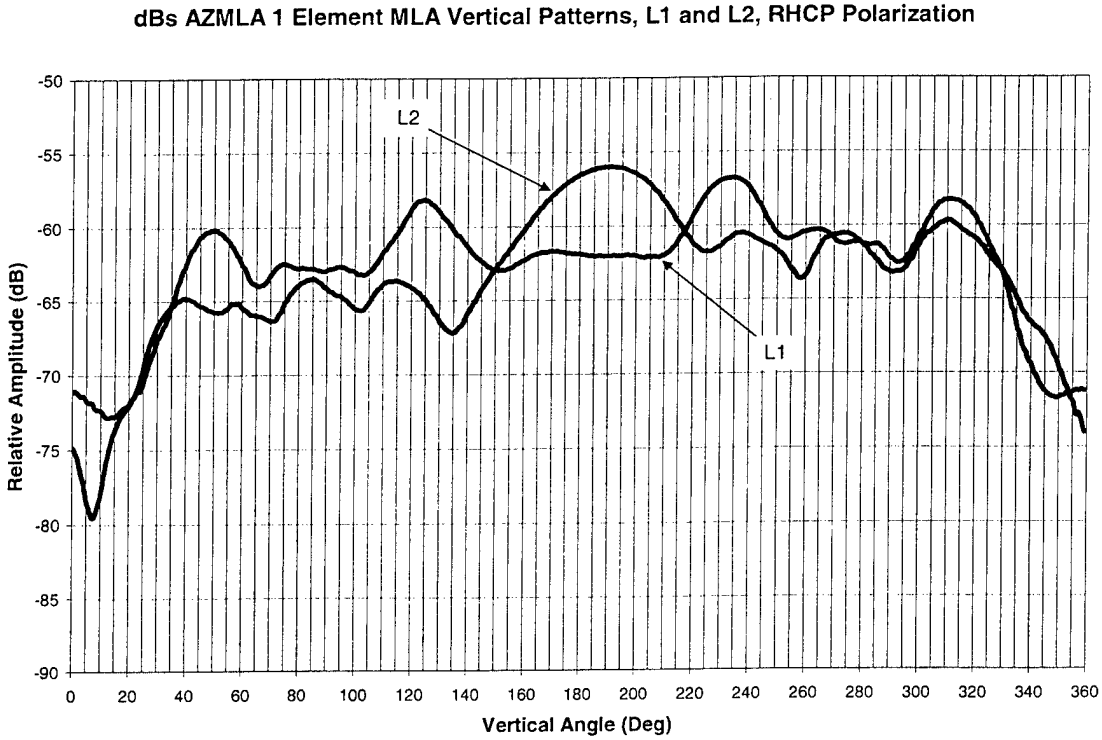

Figure 22. Single Element MLA Array Vertical Patterns at L1 and L2

- Four of Eight Cross-V Dipoles fed in the center of the radiating array. These data help quantify the effects of combining four elemental patterns of the Cross-V Dipole when located within the eight element array. The RHCP vertical patterns recorded at L1 and L2 for the four element array response are shown in Figure 23. As can be seen the four element array helps shape the vertical pattern significantly, providing increased pattern control over the service volume as well as reduced signal level below the horizon. However, significant improvements to the bandwidth and pattern control of the array are still required.

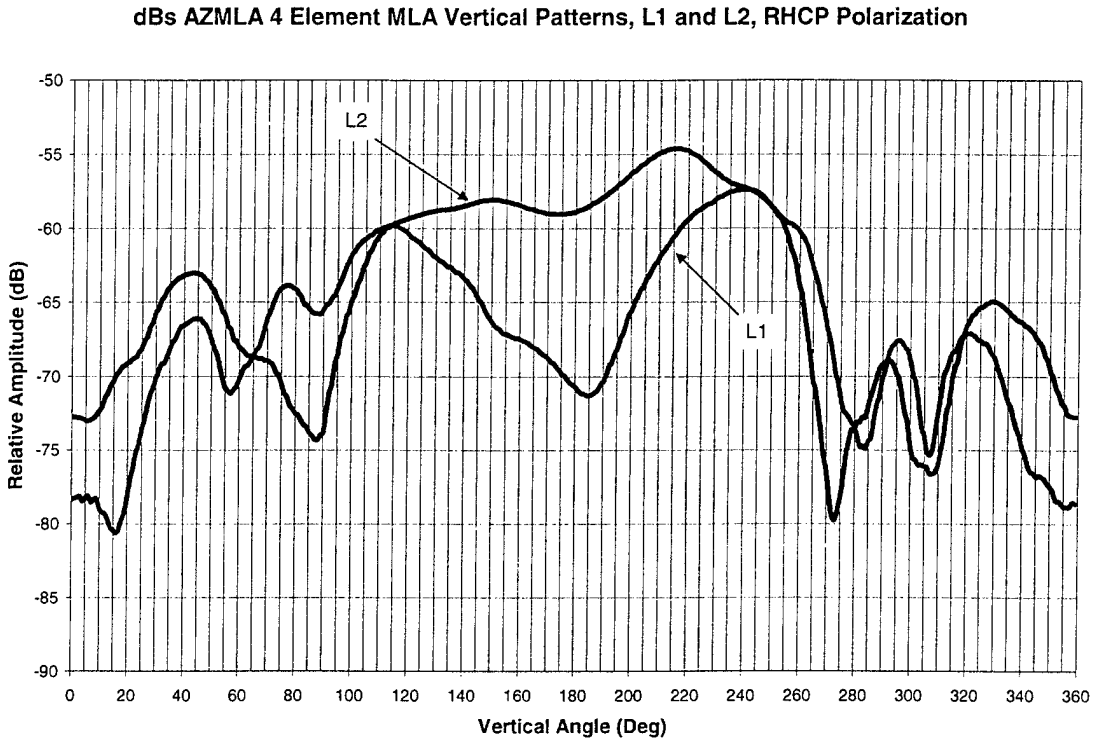

Figure 23. Four-Element MLA Array Vertical Patterns at L1 and L2

It is encouraging to see that the MLA cross-V dipole array can be shaped and formed to meet prescribed pattern response. This pattern formation is proving difficult as the basic single element pattern of the cross-V dipole does not provide as smooth a pattern as desired. The next phase of this development program will focus on the precise synthesis and formation of an MLA beam shape, which will combine correctly with the HZA pattern as well as highly suppress the negative angle energy while creating a suitable above the horizon gain pattern.

6.2.2.5 *RF Carrier Horizontal Radiation Patterns of the MLA Portion of the AZMLA*

The horizontal (i.e., azimuth) radiation pattern response of the cross-V dipole is as expected and provides an omni-directional pattern in the azimuth plane. The horizontal plane amplitude response is uniform for a cross-V dipole and the phase exhibits the expected 360 deg linearly increasing phase shift as a function of azimuth angle.

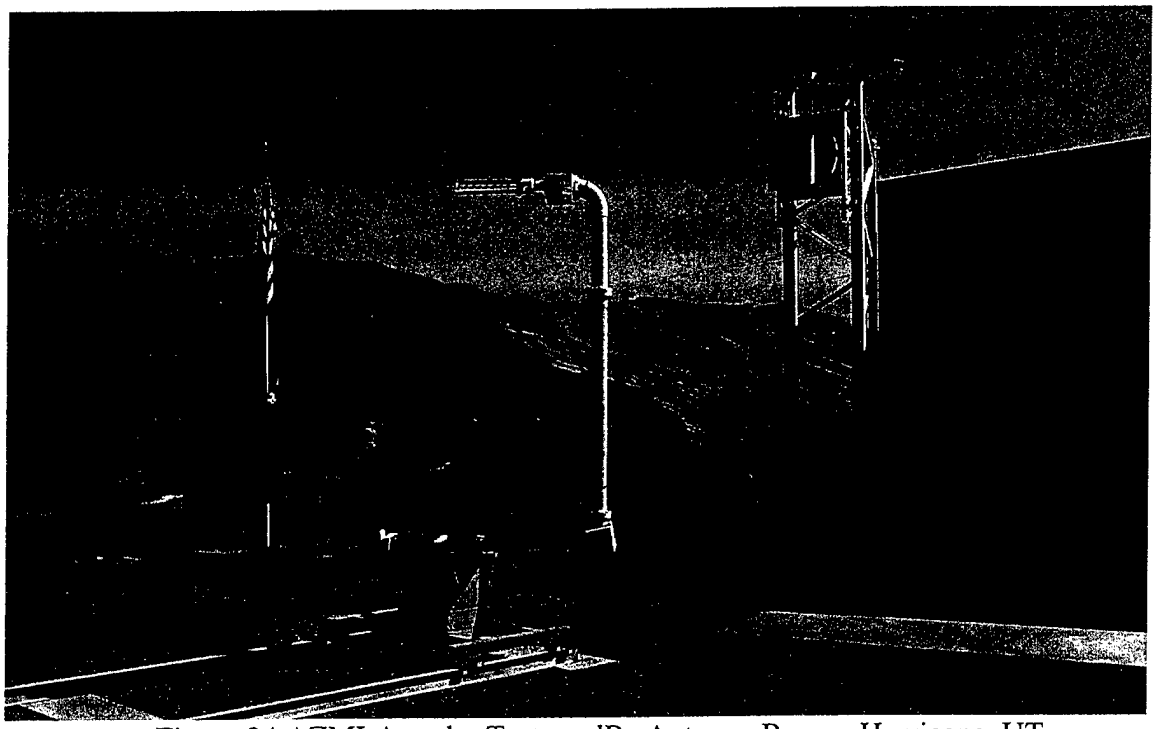

Figure 24 AZMLA under Test on dBs Antenna Range, Hurricane, UT

6.2.3 *HZA Portion of AZMLA*

The vertical RF Carrier patterns for the High Zenith Antenna have been measured at L1 (1575 MHz) and L2 (1227 MHz). Photos of the HZA are shown in Figures 25. Several configurations of the HZA have been prototyped and tested. The configuration shown herein exhibits the optimum performance for the combination array of the HZA and the MLA. It exhibits good frequency response as well as reduced size to limit the resulting diameter of the AZMLA when housed in a single cylindrical fiberglass radome.

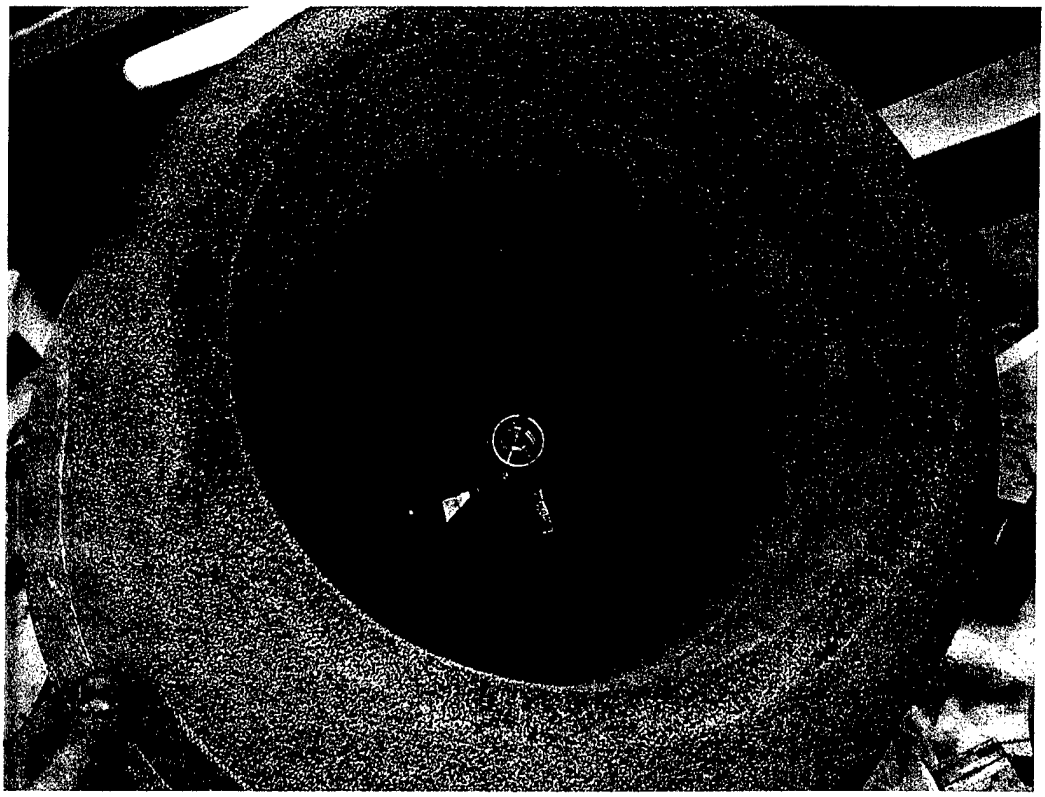

Figure 25. HZA Top View Showing Cross-V-Dipole Radiator

6.2.3.1 *RF Carrier Vertical Radiation Patterns of the HZA*

The RHCP vertical (i.e., elevation) radiation pattern response of the HZA is shown in Figure 26. As can be seen, the HZA provides good high-zenith coverage as well as very good negative-angle sidelobe suppression. Once the vertical patterns of the MLA portion of the AZMLA are working, the HZA pattern will be added to the MLA pattern to form the complete AZMLA hemispherical pattern. The addition of the HZA pattern to the MLA pattern will fill any residual high-zenith nulls which are present in the MLA's vertical pattern.

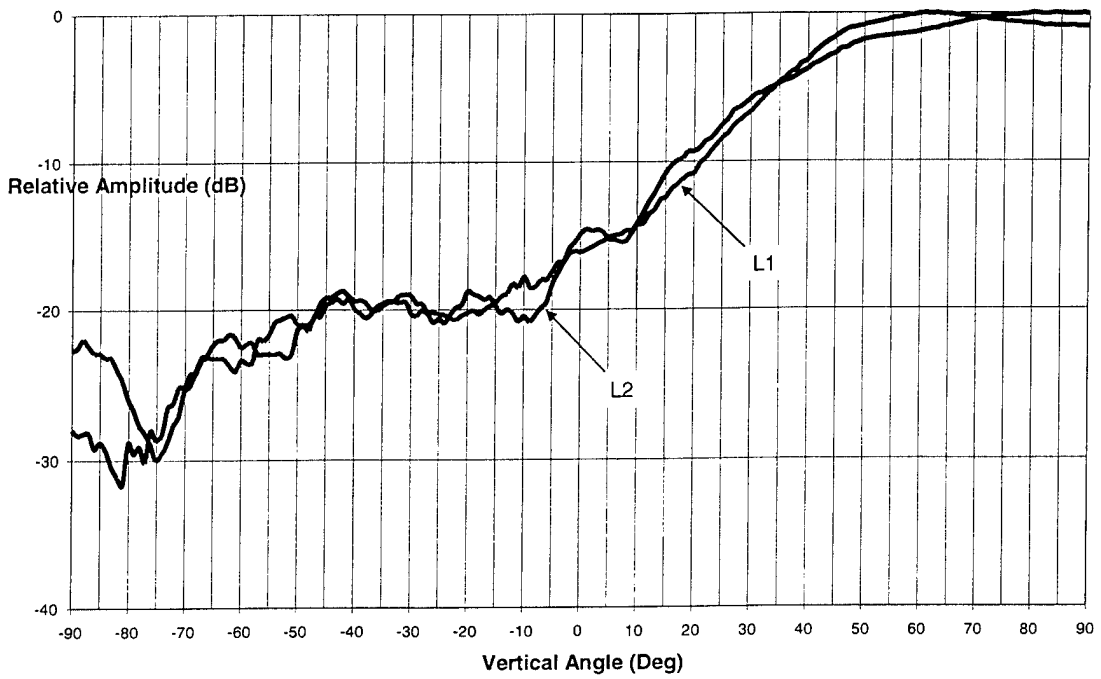

Figure 26. RHCP Vertical Patterns for the HZA

6.2.4 *Combined HZA AND MLA RF Radiation Patterns to form the AZMLA*

When properly combined the patterns of the MLA and HZA antennas will provide hemispherical coverage with high gain and low negative-angle energy (high D/U ratio). The two antennas have still not been combined to produce a complete hemispherical antenna. The HZA pattern, however, has been combined with the theoretical performance of the MLA resulting in the hemispherical performance shown in Figure 27. It is not yet known how close the actual MLA pattern will resemble the theoretical MLA.

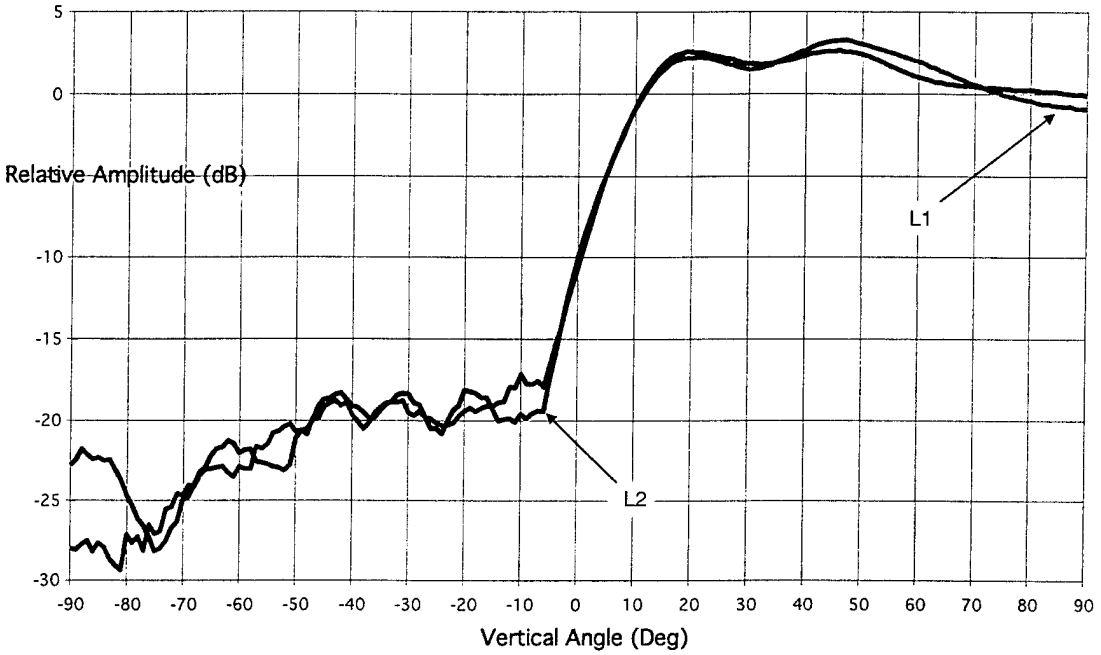

Figure 27. Theoretically Combined HZA and MLA Patterns

6.2.5 *Conclusions and Recommendations for the AZMLA*

The AZMLA as described herein holds promise to become a mid-range performing multipath limiting GPS/PL antenna, which can simultaneously operate at both L1 and L2 frequencies.

Accurate phase/amplitude response at this very broad band frequency requirement is difficult and will limit the achievable sidelobe suppression and associated D/U ratio.

Preliminary testing of the four-element cross-V-dipole MLA array indicates that the MLA array alone, without the use of the HZA, may be able to provide the desired hemispherical pattern response. This would significantly simplify the AZMLA design as well as make it smaller and lighter. It does, however, add difficulty to the design and synthesis of the MLA array. The current ability of the array to fill the high zenith null only exists over a portion of the operating frequency band. As can be seen in Figure 23, the high zenith null is filled at L2 but not at L1.

The technical difficulty of the AZMLA development has been great While still promising, the resulting performance does not meet the original design envelopes. Control over the vertical patterns of the MLA portion of the AZMLA has proven to be complicated when applying the broad bandwidth requirements upon the array. The design of an adequate cross-V dipole which allows vertical stacking of multiple elements to form a co-linear vertically stacked array has also been complex. The mechanical layout of the power distribution assembly in a manner which does not affect the radiation response of the cross-V

dipole is problematic. As can be seen in Figure 19, the current approach is to locate the coaxial cables which feed each element along the outer perimeter of the central support structure. The required 90-deg hybrid which must be located at the feed point of each element drives the mechanical size of the center support tube which in turn has an effect on the radiation characteristics of the element. Successful development of the AZMLA is still believed to be possible with effort. Further development of the AZMLA is still favorable given that there is a significant application for an antenna with the performance planned for the AZMLA. Continued development would be well worth the additional effort required to complete it.

7. CONCLUSIONS

This final report documents activities performed under contract F29601-00-C-0212, for the functional requirements and technical assessment for the development of an ANTS using the GPS. Under the Base Year of this contract, an FLSS Architecture Study was performed. Under Option Year 1, Technology Assessment items: 1) GPST, and 2) a small AZMLA were developed. This report documents the outcome from these activities.

Under the FLSS, the ANTS functions are partitioned into GS, AS, and an SS. The ANTS system operates in four primary and five auxiliary modes. The four primary modes are: 1) Mode 1: Differential GPS (DGPS), 2) Mode 2: DGPS / DPL, 3) Mode 3: PL-Only (non-differential, with no GPS at some point), and 4) Mode 4: DPL (no GPS at some point).

After the ANTS FLSS was largely completed, an Architecture Trade-off Analysis was conducted. A GPS (L1, L2 C/A and/or P-Code) and INS integrated system was used as a baseline configuration. This baseline configuration was used to assess if additional performance can be attained for an ANTS. The analysis was largely performed by a Simulation Model using GPS, INS, and PLs with an Extended Kalman Filter. The simulations performed modeled an AS trajectory of approximately 535 seconds (8.92 minutes), which uses a 0.7 nm/hr medium accuracy INS and conservative 4-channel P-Code GPS receiver. An additional four ground-based PL measurements were simulated to provide additional extended Kalman filter measurement updates. Depending on the radial distance of the PL measurements and actual Kalman filter implementation onboard the AS, how the Kalman filter measurements are implemented, and if the PL measurements are available, as simulated in this project, a reduction of horizontal error between 24.6% and 94.7% may be expected with 68% confidence. Also, altitude error was found to be associated by two factors: a) the radial distance of the PLs, and b) the orientation of the PLs with respect to the AS trajectory. Results showed that altitude error reduction of 38.8% and 82.8% may be expected at 68% confidence, given an optimal onboard (i.e., AS) Kalman filter integration. Because of the vehicle dynamics, it is critical that the Kalman filter tuning and measurement update rates, including the overall systems integration of the automated flight controls, be adjusted accordingly to ensure navigation, guidance and control optimization. The final seconds of AS flight (while the space-based GPS is assumed to not be available are critical to obtain good system performance for the ANTS.

The GPST was formed by integrating an IN500 PL transmitter, a NovAtel Millennium GPS/PL receiver, RF attenuator/blanker circuit, and real-time controller, which is autonomous and re-configurable. A prototype GPST was developed for applications evaluation in the ANTS and for technology assessment. Due to contractual difficulties the secondary source was selected for the PL transmitter. This secondary source, IntegriNautics, Incorporated, provided a larger, highly capable box (IN500) but was L1 C/A and P-code only; it did not generate L2. To overcome this shortcoming, an L1-to-L2 translator was designed, built, and tested. The dual-frequency nature of the PL transmitter was used primarily to achieve the desired frequency diversity during scenarios where only one of the two GPS frequencies was unavailable. These PL signals can then be used to augment the GPS SV constellation or be used as a separate ranging source. A low power version of the attenuator/blanker circuit was designed and built which illustrated some timing issues associated with the real-time control of this function. Additional resolution is need to ensure a small time slice (356 ns) of high power that may trigger the AGC loops within the GPS/PL receivers internal to the GPST. Good system performance was attained on L1 and L2, C/A and P-code tracking.

Although the overall AZMLA is not complete and did not met the overall design envelope initially sought, the AZMLA still holds promise to become a mid-range performing multipath limiting GPS/PL antenna which can simultaneously operate at both L1 and L2 frequencies. Accurate phase/amplitude response at this very broad band frequency requirement is difficult and will limit the achievable sidelobe suppression and associated D/U ratio. Preliminary testing of the 4 element cross-V-dipole MLA array indicates that the MLA array alone may be able to provide the desired hemispherical pattern response, which would significantly simplify the AZMLA design, as well as, make it smaller and lighter. Control over the vertical patterns of the MLA portion of the AZMLA has proven to be complicated when applying the broad bandwidth requirements upon the array. The design of an adequate cross-V dipole, which allows vertical stacking of multiple elements to form a co-linear vertically stacked array has also been complex. The mechanical layout of the power distribution assembly in a manner which does not affect the radiation response of the cross-V dipole is problematic. Successful development of the AZMLA is still believed to be possible with effort. Further development of the AZMLA is still favorable given that there is a significant application for an antenna with the performance planned for the AZMLA.

The objective of this program was to provide sufficient assessment for the potential development of an ANTS that will minimize the risk for successful implementation of the final ANTS in the future. Emphasis was proposed and placed on the purchase of COTS equipment whenever practical available. The FLSS and the Architecture Trade-off Analysis, although not exhaustive, did provide sufficient detail and illustrated the potential benefit to an ANTS. The GPST developed provided sufficient detail to see the benefit of an integrated GPS-like (i.e., PL) transmitter and GPS/PL receiver package. The deployment of ground-based PL transmission and reception assets would require a transportable antenna system to mitigate multipath; the AZMLA was a goal of this capability that was not achieved, but did provide sufficient technology assessment of the small-stacked array technology prototyped. While the overall design predicts good performance, fabrication difficulties existed in terms of mutual coupling between array elements which limited its overall performance.

For this contractual effort, an FLSS, architecture analysis and technology assessments of key items necessary for ANTS deployment were performed. Several innovative techniques which were explored include the development of a GPST, their integration in multiple GSUs, and the development of a small AZMLA technology. As stated in the original proposal, all of the major items in the program are "pushing" the state-of-the-art with respect to the fact that, to the best of our knowledge, they are not being done elsewhere. Successful implementations of these techniques will have direct impact on the potential future deployment of an ANTS. Additional risk mitigation would likely be required to ensure this successful implementation.

8. REFERENCES

[1] Contract between U.S. Air Force and Ohio University, F29601-00-C-0212, dtd December 2000.

[2] ADVANCED NAVIGATIONAL TERMINAL SYSTEM (ANTS) USING THE GLOBAL POSITIONING SYSTEM, Functional Level Systems Specification Document, Avionics Engineering Center, Ohio University, August 2002.

[3] Gray, R., GPS ANTI-JAM, A Missile Simulation Model using INS, GPS and Ground Based Pseudolites with an extended Kalman filter, Project Report, ERI-Systems, June 21, 2002.

[4] Gray, Robert and Peter Maybeck Gray, R. An Integrated GPS/INS/BARO and Radar Altimeter for Aircraft Precision Approach Landings. IEEE National Aerospace Conference. pp. 1-8 (1995).

[5] Mosle, William B. *Detection, Isolation, and Recovery of Failures in an Integrated Navigation System.* MS Thesis, AFIT/GE/ENG/93D-28. School of Engineering, Air Force Institute of Technology, Wright-Patterson AFB OH, December 1993 (AD-A274056).

[6] Snodgrass, Faron Britt. *Continued Development and Analysis of a New Extended Kalman Filter for the Completely Integrated Reference Instrumentation System (CIRIS).* MS Thesis, AFIT/GE/ENG/90M-5. School of Engineering, Air Force Institute of Technology (AU), Wright-Patterson AFB OH, March 1990 (AD-A220106).

[7] Stacey, Richard D. *A Navigation Reference System (NRS) Using Global Positioning System (GPS) and Transponder Aiding.* MS Thesis, AFIT/GE/ENG/91M-04. School of Engineering, Air Force Institute of Technology, Wright-Patterson AFB OH, March 1991 (AD-A238890).

[8] Vasquez, Juan R. *Detection of Spoofing, Jamming, or Failure of a Global Positioning System (GPS).* MS Thesis, AFIT/GE/ENG/92D-37. School of Engineering, Air Force Institute of Technology, Wright-Patterson AFB OH, December 1992 (AD-A259023).

[9] Musick, Stanton H. *PROFGEN - A Computer Program for Generating Flight Profiles.* Technical Report, Air Force Avionics Laboratory, WPAFB, OH, November 1976. AFAL-TR-76-247, DTIC ADA034993.

[10] Aeronautical Systems Division, AFSC. *Specification for USAF Standard Form, Fit and Function (F3) Medium Accuracy Inertial Navigation Unit, F-16 Aircraft Application.* NU84-1/F-16, Revision A, Change Notice 1, Wright-Patterson AFB, OH, 20 Aug 1991.

[11] Knudsen, L. *Performance Accuracy (Truth Model/Error Budget) Analysis for the LN-93 Inertial Navigation Unit.* Technical Report, Litton Guidance and Control Systems, Woodland Hills, CA, January 1985. DID No. DI-S-21433 B/T:CDRL No. 1002.

[12] Musick, Stanton H., and Neil Carlson. *User's Manual for a Multimode Simulation for Optimal Filter Evaluation (MSOFE).* AFWAL-TR-88-1138, Wright-Patterson AFB OH: A.F. Avionics Laboratory, AFWAL/AARN-2, April 1990.

[13] Bartone, C.G., and Van Graas, F., "Airport Pseudolite for Precision Approach Applications, *Proceedings from the Institute of Navigation-GPS-97*, September 16-19, 1997, pp. 1843-1849.

[14] Bartone, C.G., and Van Graas, F., "Ranging Airport Pseudolite for Local Area Augmentation", *The Institute of Electrical and Electronics Engineers (IEEE), Position,. Location, and Navigation Symposium (PLANS)*, IEEE Catalog Number: 98CH36153, April 20-23, 1998, pp. 479-486.

[15] Bartone, C.G., "Multipath Considerations for Ground Based Ranging Sources", *Proceedings from the Institute of Navigation-GPS-99*, September 16-19, 1999.

[16] Bartone, C.G., "Development of a Wideband Airport Pseudolite for GPS Augmentation", *Proceedings from the Institute of Navigation-National Technical Meeting*, January 25-28, 2000.

[17] Bartone, C.G., and Van Graas, F., Airport Pseudolite for Local Area Augmentation", *Institute of Electrical and Electronics Engineers, Transactions on Aerospace and Electronics Systems*, planned publication date is 1/00.

[18] Kiran, S., Bartone, C.G. "Wideband Airport Pseudolite for the Local Area Augmentation System", IEEE PLANS, April 2002.

[19] Thornburg, B., et.al., "An Integrated Multipath Limiting Antenna for the Local Area Augmentation System", *Proceedings from the Institute of Navigation-GPS-02*, September 25-27, 2003.

[20] Thornburg, B., "In-Process Report for All-Zenith Multipath Limiting Antenna Program, dB Systems, Inc., June 12, 2003.

DISTRIBUTION LIST

DTIC/OCP 8725 John J. Kingman Rd, Suite 0944 Ft Belvoir, VA 22060-6218	1 cy
AFRL/VSIL Kirtland AFB, NM 87117-5776	2 cys
AFRL/VSIH Kirtland AFB, NM 87117-5776	1 cy
Official Record Copy AFRL/VSEB/Sandra Slivinsky	2 cys